The role of intermediate-depth currents in continental shelf–slope accretion: Canterbury Drifts, SW Pacific Ocean

R. M. CARTER

Marine Geophysical Laboratory, James Cook University, Townsville, Qld. 4811, Australia (e-mail: bob.carter@jcu.edu.au)

Abstract: The Late Oligocene to Recent Canterbury Drifts were deposited in water depths between *c*. 400 and *c*. 1500 m by northward-flowing, cold, intermediate-depth water masses: Subantarctic Mode Water (SAMW), Antarctic Intermediate Water (AAIW) and their predecessor current flows. Drift accumulation started at *c*. 24 Ma, fed by terrigenous sediment derived from the newly rising Alpine Fault plate boundary in the west, which has built a progradational shelf–slope sediment prism up to 130 km wide at rates of eastward advance of up to 5.4 km Ma^{-1}. Gentle uplift associated with the nearby plate boundary has exposed older Late Oligocene and Miocene drifts onland (Bluecliffs Formation). Ocean Drilling Program Site 1119, located 100 km offshore at a water depth of 394 m, penetrated a 428 m thickness of mid-Pliocene to Pleistocene (0–3.9 Ma) drift located just seaward of the eastern South Island shelf edge. Uniquely, these large (>60 000 km^3), regionally extensive, intermediate-depth sediment drifts can be examined in outcrop, in marine drill-core and at the modern sea bed. The drifts comprise planar-bedded units up to several metres thick. Some sand intervals have sharp, erosive bases and normally graded tops into overlying siltstone; others are symmetrically graded with reverse-graded bases and normally graded tops. Bioturbation is moderate and rarely destroys the pervasive background, centimetre-scale, planar or wispy alternation of muddy and sandy silts displayed by Formation Micro-Scanner imagery. These features are consistent with deposition from rhythmically fluctuating bottom currents. Texturally, the drifts are polymodal quartzofeldspathic silty sands, sandy silts, silts and silty clays, with varying admixtures of benthic and biopelagic carbonate and silica. Miocene samples are mostly dominated by coarse silt (45–60 μm) and very fine sand (70–105 μm) grain-size modes, whereas strong fine silt (11–13 μm) and very fine silt–clay (<5 μm) modes become dominant after *c*. 3.1 Ma in the Late Pliocene, consistent with an increasing input of glacially ground material. Over the Plio-Pleistocene part of the succession, the sand–silt lithological rhythmicity occurs in synchroneity with Milankovitch-scale climate cycling, with periods of inferred faster current flow (sand intervals) mostly corresponding to warm, interglacial periods. Northward drift dispersal has helped cause the seaward growth of the eastern South Island shelf–slope system since the Late Oligocene probably by clinoform progradation and by episodic welding of mounded slope drifts onto the pre-existing sediment prism. Such along-slope, contourite drift accumulation occurs even in the absence of mounded drifts on seismic profiles, and represents a previously underemphasized mechanism for the progradation of shelf–slope clinoforms, worldwide. The Canterbury Drifts vary in thickness from *c*. 300 m near the early Miocene shoreline, where they were accumulating in limited shallow-water accommodation, to *c*. 2000 m under the modern shelf edge. Mounded drifts first occur in the Middle Miocene, at *c*. 15 Ma, their appearance perhaps reflecting more vigorous intermediate water flow consequent upon the worldwide climatic deterioration between 15 and 13 Ma. At Site 1119, a further change from large (>10 km wide) to smaller (1–3 km wide) mounded slope drifts occurs at *c*. 3.1 Ma, marking further cooling and perhaps the inception of discrete SAMW flows and initiation of the Subantarctic Front.

The concept that deep ocean currents play a major role in shaping the continental slope originated from seismic observations of migratory abyssal sediment waves (Ballard 1966; Lonsdale & Hollister 1979), and sea-bed photographs of nearby current-influenced bedforms. Similar features were later shown to occur worldwide beneath the path of contour-hugging thermohaline currents (e.g. Ewing *et al.* 1971; Hollister *et al.* 1974; Gardner & Kidd 1987; Howe *et al.* 1997), and also laterally to turbidity-current pathways (e.g. Damuth 1979; Normark *et al.* 1980; Carter *et al.* 1990). The accompanying 'contourite' sediments, with characteristic sand–mud sedimentary structures and textures (Stow & Lovell 1979), have been described both from sea-bed cores and from ancient sedimentary basins (summarized by Stow *et al.* 1998). Long Deep Sea Drilling Project (DSDP) core samples through well-known sediment drifts, the Hatton, Gardar and Feni sediment drifts in the North Atlantic, were described by Laughton *et al.* (1972), Montadert *et al.* (1979), McCave *et al.* (1980) and Kidd & Hill (1987).

From: VIANA, A. R. & REBESCO, M. (eds) *Economic and Palaeoceanographic Significance of Contourite Deposits*. Geological Society, London, Special Publications, **276**, 129–154.
0305-8719/07/$15.00

The 1980s saw a widening interest in marine sediment drifts, extending to include those developed in shallower intermediate water depths. The Faro Drift, a 300 m thick, 50 km long body located at depths of 500–700 m along the path of the deep Mediterranean outflow in the eastern Atlantic ocean (Faugères *et al.* 1984; Stow *et al.* 1986; Nelson *et al.* 1993), was a subject of particular study about the time that the first detailed facies models for drift sediments were emerging (Stow *et al.* 1998; Viana *et al.* 1998). Although it was implicit in many papers that the deposition of sediment drifts helped build up the continental margin (for instance, McCave & Tucholke (1986) referred to the 'plastering and decorating' of the sides of the North Atlantic Ocean basin), most previous research has been focused on the description of drift geometry and sedimentary facies, and the inference of current pathways.

Latterly, it has become apparent that some drift deposits play a determining role in the progradational building of the continental shelf and slope (Fulthorpe & Carter 1991; Seranne & Abeigne 1999). This paper discusses the sedimentary texture, composition, structure and origin of one such field of drifts, cored to a depth of 513 m (*c*. 3.9 Ma) offshore at Ocean Drilling Program (ODP) Site 1119 (Carter *et al.* 1999). Site 1119 is located at 394 m water depth on the upper continental slope, about 100 km east of Timaru, New Zealand (Fig. 1a and b). The sediments there represent the most recent part of a long-lived, *c*. 24–0 Ma, succession of terrigenous drifts that underlie the eastern South Island coastal plain–shelf–slope sediment prism (Fig. 2) (Carter, R. M., *et al.* 1996) and form an important part of the Eastern New Zealand Oceanic Sedimentary System (ENZOSS; Carter, L., *et al.* 1996).

This paper summarizes the available published information on the Canterbury Drifts, both offshore (ODP Site 1119) and onland (Bluecliffs Formation). New sediment textural analyses provide insights into the evolution of the drift succession since the Early Miocene, and comparison between onshore and offshore sites contributes to our understanding of the climatic and oceanographic history of the region.

Sediment analyses were conducted according to the laboratory protocols described in the Appendix. For discussion, textural data have been aggregated into three grain-size classes, cohesive mud (cM; <8.70 or <9.48 μm), sortable silt (sZ; <60.65 or <56.09 μm) and sand (sS; >60.65 or >56.09 μm). These classes represent the bin-boundary grain diameters on the laser particle sizer that, for the 2000 or 600 mm lenses, respectively, approximate to the conventional cohesive–noncohesive and silt–sand boundaries of *c*. 10 and 62.5 μm. It should be noted also that the non-specific allocation of clay–very fine silt modes to <5 or <10 μm is because these grain sizes fall at the lower end of the Mastersizer grain-size spectrum (using, respectively, the 600 or 2000 mm lens), the accuracy of mode identification in these ranges being degraded by instrumental edge effects.

Previous research on the Canterbury Drifts

Seismic delineation

The Pliocene–Recent Canterbury Drifts (Fulthorpe & Carter 1991) were deposited on the mid–upper slope east of South Island New Zealand, in depths of *c*. 400–1500 m from north-travelling Subantarctic Mode Water (SAMW) and Antarctic Intermediate Water (AAIW), and their predecessor water masses (Fig. 2). The drifts were first imaged on reconnaissance petroleum exploration seismic lines shot by Gulf (1973), and their widespread regional distribution was revealed by a detailed seismic survey of the offshore Canterbury Basin (Western Geophysical 1982). Small, upslope-migrating sediment drifts are also known to occur on the modern sea bed in the head of the Bounty Trough (Fig. 1c), but remain undescribed in detail.

Using the Western Geophysical seismic database, Fulthorpe & Carter (1991) showed that deposition of the offshore Canterbury Drifts has played a pivotal role in the seaward progradation of the continental shelf sediment prism since at least the Late Miocene. Drifts initially form on the slope at depths several hundred metres below the shelf edge, from which they are separated by a channel-like, longitudinal gutter, and build up alongshope and shorewards (west) under the influence of the Coriolis effect. Once the crest of a drift approaches the same depth as the continental shelf edge, sediment aggradation fills the intervening gutter. Thereby, the seaward part of the crest of the drift comes to mark a new shelf edge. By this process, the shelf edge intermittently vaults seawards across the gutter and half the width of the newly emplaced drift (5–15 km) in a single step (see Fig. 3a).

An extensive grid of new high-resolution multichannel seismic profiles through the Canterbury Drifts was collected during R.V. *Maurice Ewing* cruise EW00-01 in 2000. These data, the upper parts of which have a resolution of *c*. 5 m, have been analysed by Lu *et al.* (2003) and Lu & Fulthorpe (2004), who described the 3D shape of what they termed elongate, complex and subsidiary drifts. Those workers recognized 11 major drifts within the younger, Late Miocene–Pleistocene part of the Otakou Group, and established a detailed model for their deposition.

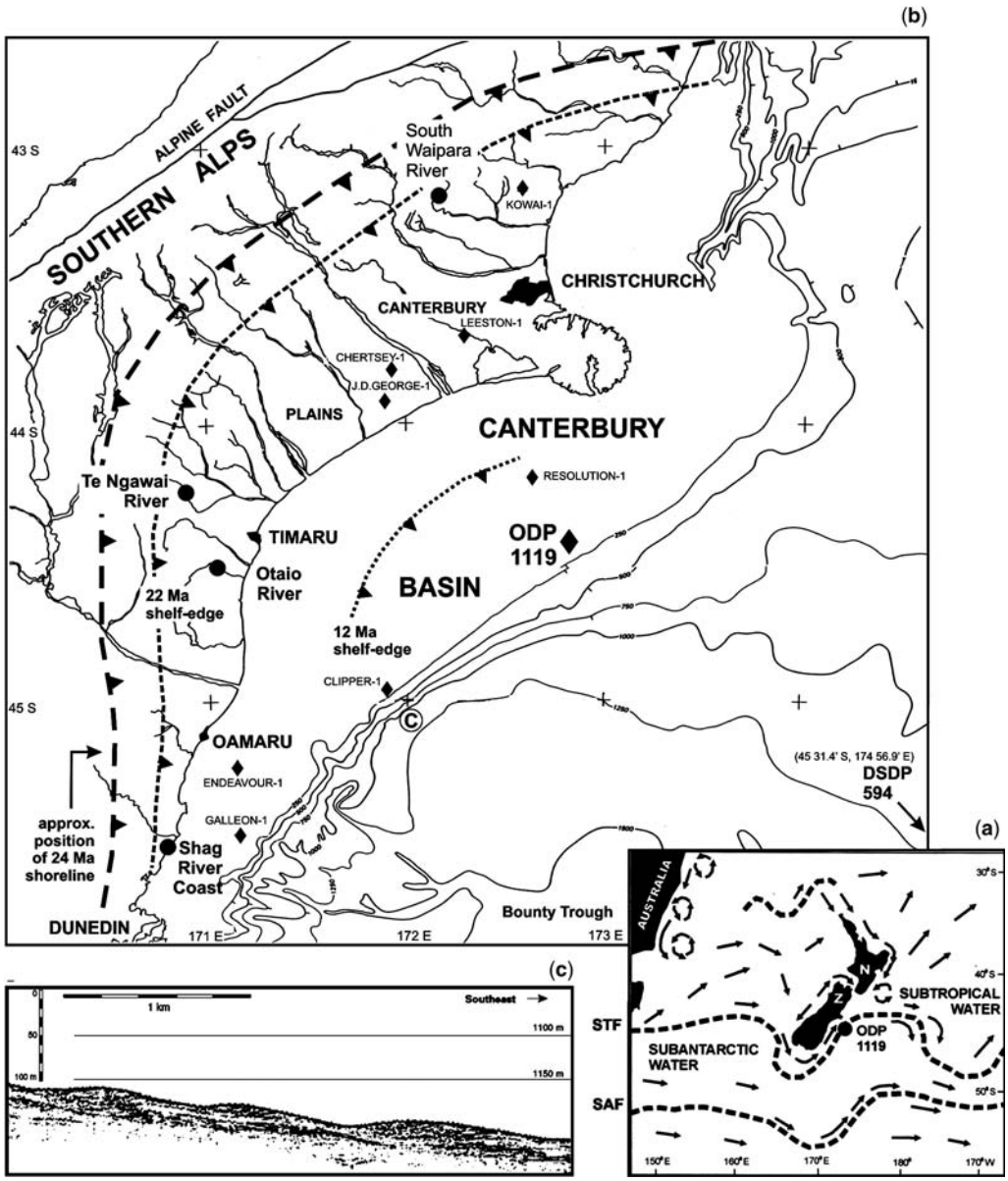

Fig. 1. (**a**) Regional oceanographic setting for the New Zealand region, showing the disposition of modern surface current flows and fronts. STF, Subtropical Front; SAF, Subantarctic Front. (**b**) Central and eastern South Island, showing location of the Canterbury Basin, ODP Site 1119, petroleum drill-holes and important localities for onland drifts of the Bluecliffs Formation. Bold dashed line indicates the Late Oligocene (24 Ma) position of the western edge (shoreline) of the Canterbury Basin at the commencement of regression and eastward shelf–slope progradation; the approximate position of the shelf-edge at *c*. 22 and *c*. 12 Ma are also indicated. (**c**) A 3.5 kHz profile downslope and SW of ODP Site 1119, showing small (1 km spaced) modern sediment drifts at a water depth of 1100 m (location marked, as **c**, in (**b**)).

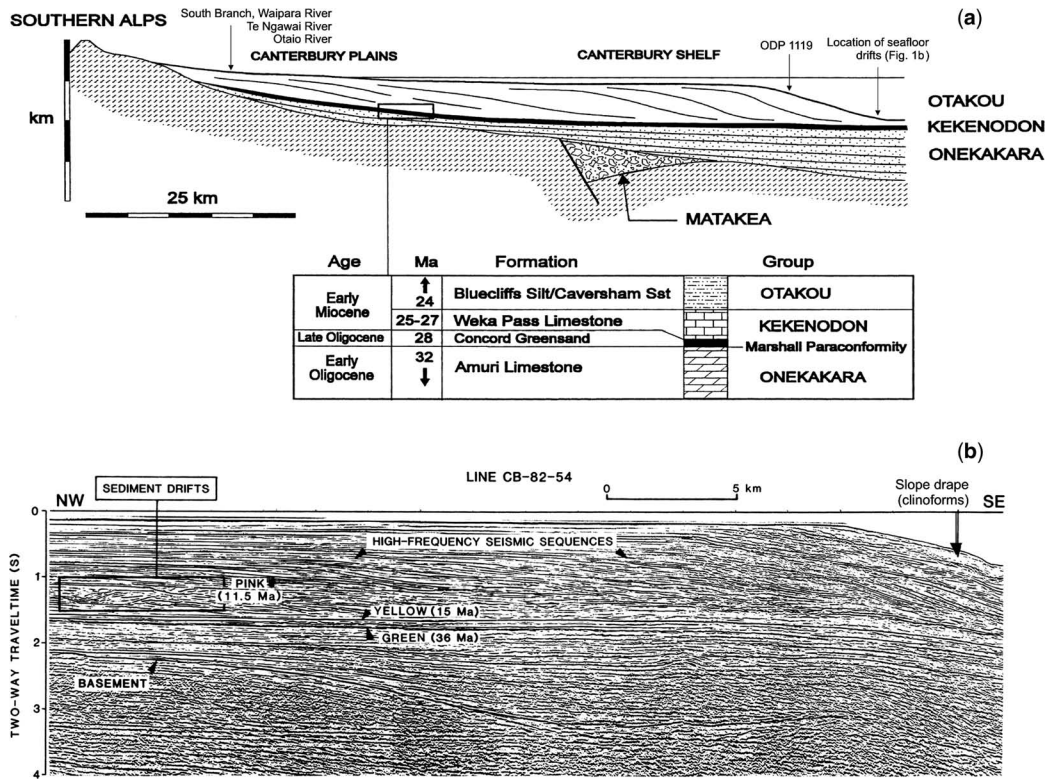

Fig. 2. (**a**) Schematic west–east profile across the Canterbury Basin. Late Cretaceous, post-Gondwanan rifting (rift-fill Matakea Group) was followed by thermal subsidence and marine transgression until the Early Oligocene (onlapping Onekakara Group). At *c.* 33.5 Ma, opening of the Tasman Rise gateway far to the SW caused the establishment of strong proto-Circum Antarctic Current flows across the largely (Fleming 1962) or completely (LeMasurier & Landis 1996) submergent New Zealand Plateau, causing the formation of a regional paraconformity (Marshall Paraconformity) followed by current-emplaced deposition of greensands and bioclastic carbonates (oceanic plateau, Kekenodon Group). Uplift on the Alpine Fault plate boundary commenced in the Late Oligocene (*c.* 25 Ma), the yield of new terrigenous sediment causing the eastward progradation of the shelf–slope prism (Otakou Group). Clinoform foresets of the Otakou Group correspond onland to the Bluecliffs Formation. The Pliocene to Recent Canterbury Drifts are centred under the outer shelf and slope in the vicinity of ODP Site 1119, but mounded drifts as old as Late Miocene occur within the Otakou Group, and sediments with drift characteristics occur down to the base of the group onland. (**b**) Commercial (low-resolution) seismic line through the outer shelf and upper slope, central Canterbury Basin, showing geometry of the major stratigraphic units. Kekenodon Group is delimited by the green (below) and yellow (above) seismic reflectors (after Fulthorpe & Carter 1991).

ODP Site 1119

ODP Site 1119 provided the first drill-core through the younger part of the Canterbury Drifts, penetrating down as far as the top of Drift 10 of Lu & Fulthorpe (2004) with an age of *c*. 3.9 Ma. Carter *et al.* (1999) briefly characterized the drift succession as alternating thicker (intervals up to 10 m thick) muds and intervening thinner (intervals up to 3 m thick) sand beds. Most of the sand intervals, some of which are carbonate rich, correspond to warmer, interglacial periods when the water at the site was *c*. 100 m deeper than at glacial lowstand and the shoreline was located many tens of kilometres inboard (west) of the shelf edge. Carter *et al.* (2004*a*) showed that a number of smaller late Pliocene to Pleistocene drifts overlie the large, early Pliocene Drift D10. They interpreted the change in drift size and seismic geometry that occurred at *c*. 3.1 Ma as reflecting intensified intermediate water flow, consequent upon climatic deterioration and the development of Northern Hemisphere glaciation.

Regional distribution of drifts

Plate boundary uplift during the later Cenozoic has caused the gentle eversion of the western (landward) parts of the Canterbury Basin succession, such that Early to Middle Miocene equivalents of the Site 1119 drifts are today exposed onland as the regressive Bluecliffs Silt Formation (Gair 1959; Carter 1988). These older drifts are widely present beneath the continental shelf and coastal plain of eastern South Island, which they have materially built (Fulthorpe & Carter 1991; Lu *et al.* 2003) (see Fig. 2a). Outcrops show that the lowest part of the terrigenous drift succession is marly, with an enhanced content of biopelagic tests, consistent with its deposition immediately above, and transition from, a mid–late Oligocene greensand–carbonate facies that was deposited widely on the New Zealand mid-Cenozoic oceanic plateau (Kekenodon Group; see Ward & Lewis 1975). The marls represent the distal (seaward) toes or bottomsets of the eastward-advancing prism of terrigenous sediment.

The term Canterbury Drifts is here extended to encompass all the terrigenous sediment drifts that underlie the eastern South Island coastal plain, shelf and slope, and that range from latest Oligocene to Recent in age. These sediments display a mineralogy that reflects their origin from South Island Rangitata Synthem rocks, especially the Haast Schist (chlorite–biotite zone), and its north-flanking Torlesse metagreywacke (prehnite–pumpellyite zone) belt (e.g. Reed 1957; Craw 1984). Terrigenous sand and silt petrography is dominated by quartz, albite, epidote–clinozoisite, sericite and chlorite.

Terrigenous-silt-dominated units of Early Miocene to Pliocene age have been mapped widely across the Canterbury Basin under local names that include the Grey Marl (Hector 1877), Mt. Harris Beds (Hector 1884), Goodwood Limestone (Service 1934), Tokama Siltstone (Mason 1941), Awamoa Beds (Gage 1957), Waikari Formation (Andrews 1963), Conway Formation (Warren & Speden 1978), Waima Siltstone (Lewis *et al.* 1980) and Caversham Sandstone (Bishop & Turnbull 1996). These units, and probably also some of the younger Pliocene Greta (Hutton 1888) and Motunau (Buchanan 1870) siltstones and their equivalents, are part of the regional Bluecliffs Formation of Carter (1988) and the Canterbury Drifts as interpreted here.

Canterbury Drifts offshore (ODP Site 1119)

Stratigraphy and lithology

The topmost interval at Site 1119, unit A, 0–86.19 m composite depth (mcd), comprises sediment that has been bypassed seawards across the shelf and shelf edge to accumulate as a clinoform drape on the upper slope (Carter *et al.* 2004*b*) (Fig. 3a and b). This surficial 86 m thick interval of terrigenous muddy siltstone and muddy very fine sandstone has a sand:mud bed ratio of 1:23 and an average sedimentation rate of 36 cm ka^{-1} (Unit A; 0–0.252 Ma; MIS 1–7). Below a small 25 ka long unconformity in MIS 8, Site 1119 penetrated 428 m of similar sediments, which represent the Canterbury Drift succession *sensu stricto* (Units B–C; 0.28–3.92 Ma; MIS 8–Gi 11) (Carter & Gammon 2004). Units B2–3 exhibit lesser sedimentation rates (20 and 21 cm ka^{-1}, respectively) and higher sand:mud bed ratios (1:8 and 1:7, respectively) than the clinoform strata above. Lower in the section still, Units B4–C2 are characterized by remarkably constant sedimentation rates of *c*. 10 cm ka^{-1}, and a sand:mud bed ratio either between 1:6 and 1:8 (Units B4–B5c) or an absence of sand beds altogether (Units C1–2). Overall, Site 1119 records a total sand bed thickness of 53.92 m out of a total thickness of 513.5 m of sediment, for an average sand:mud bed ratio of 1:9.5, and the succession was deposited at water depths that shoaled from *c*. 900 to 400 m over the last 3.9 Ma.

Site 1119 cores and Formation Micro-Scanner (FMS) images (Figs 3c and 4) show that Units B and C comprise centimetre-scale-bedded, silty mudstone and muddy and sandy siltstone, variously

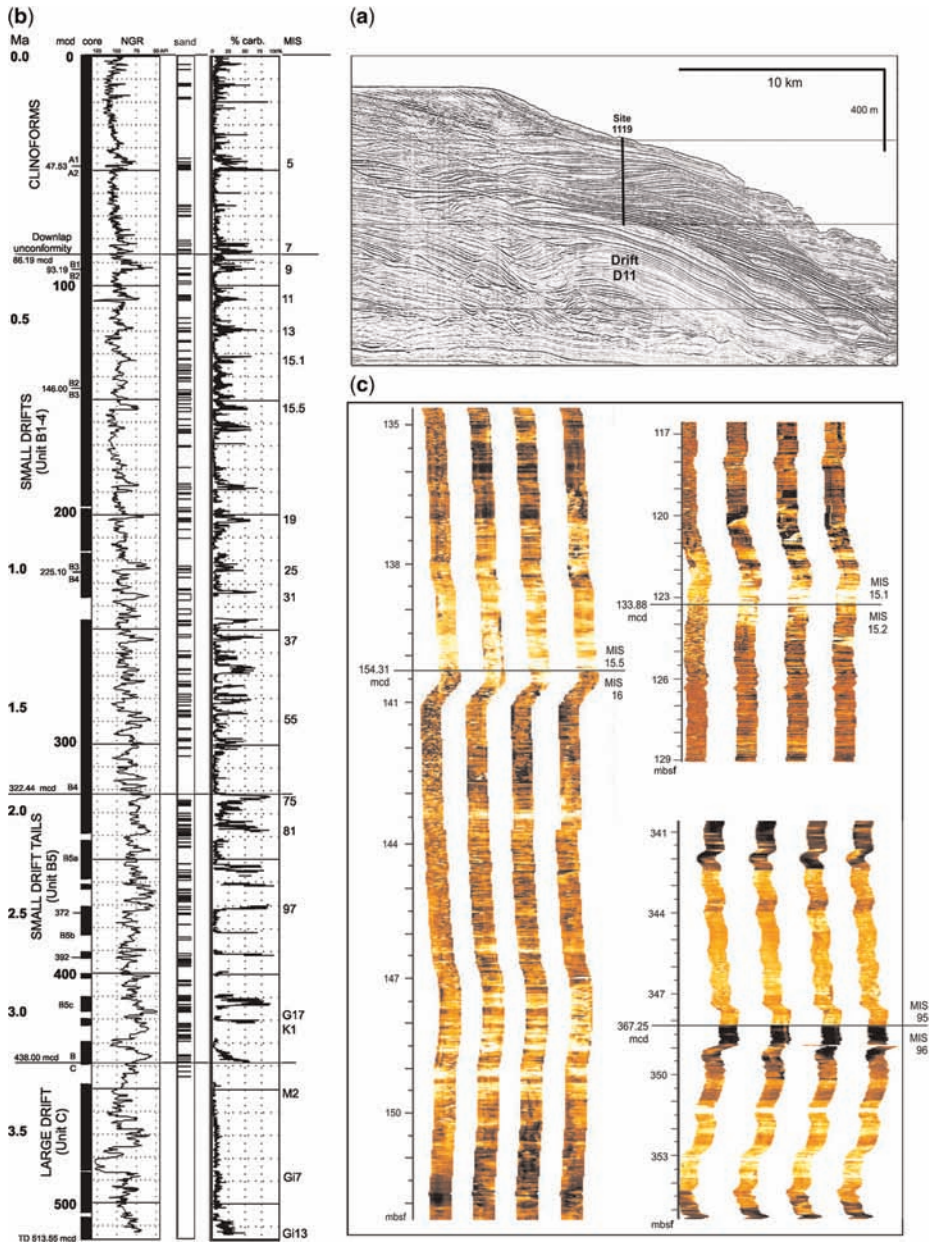

Fig. 3. (**a**) High-resolution seismic section through the Canterbury Drifts at ODP Site 1119 (courtesy C. Fulthorpe). (**b**) Stratigraphy of Site 1119. Columns, from the left, are: age (Ma), core depth in metres composite depth (mcd), core recovery (core), natural gamma-ray intensity (NGR), sand log (sand), grey-scale reflectance (% carb.) and selected Marine Isotope Stages (MIS; identified from the NGR record, after Carter & Gammon 2004). (**c**) Formation Microscanner (FMS) resistivity images of drift intervals 117–129 (unit B2), 135–152 (units B1–B2) and 341–355 m below sea floor (mbsf) (unit B5a); white and yellow indicate high resistivity (concretionary layers, sands); orange to brown, lower resistivity (sandy silts, silts); black, borehole washout. Noteworthy features area: (1) the presence of a sharp-based, normally graded sand near 140 mbsf; a sharp-based and sharp-topped sand between 343 and 348 mbsf; rhythmic double-graded sand intervals centred near 123, 143 and 148 mbsf; (2) the pervasive background presence of undulose, centimetre-scale, interbedded coarser and finer silts.

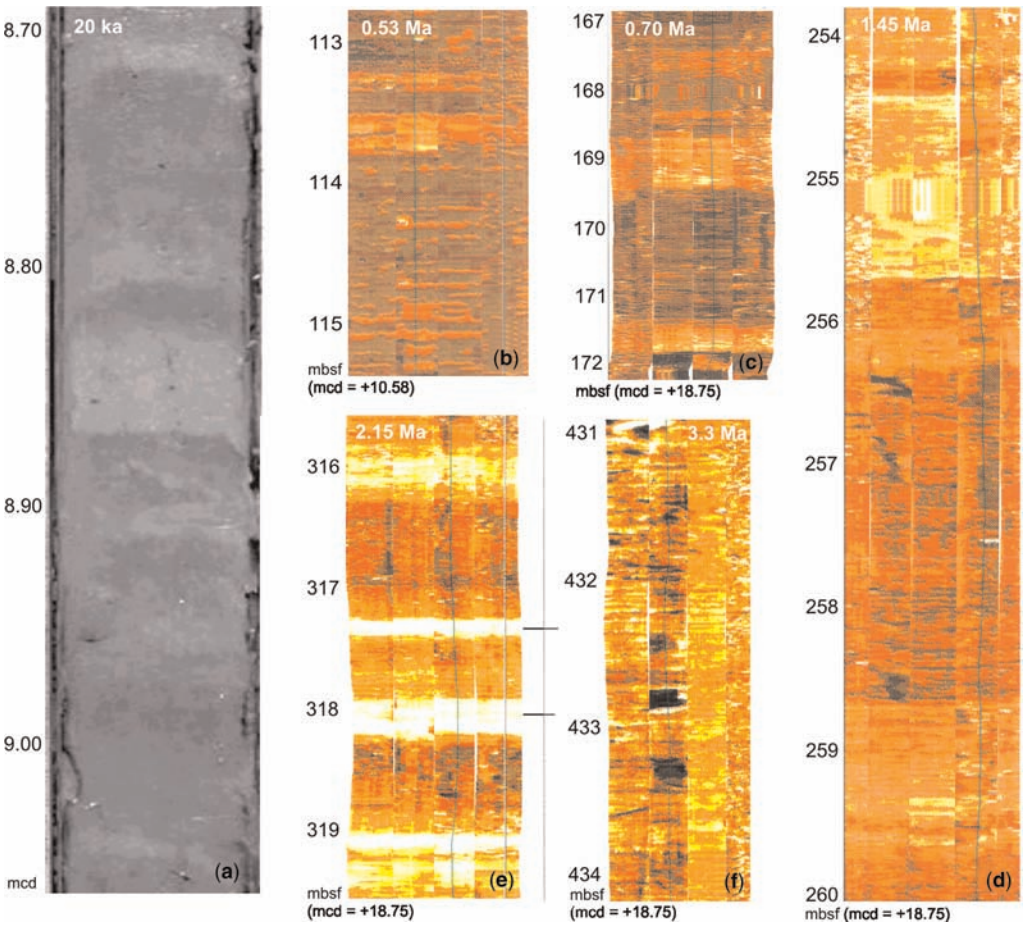

Fig. 4. Images from core 1119C. (**a**) Core photograph from the interval 8.70–8.10 mcd, showing interbedded, slightly burrowed, light and dark muds deposited during the last glacial maximum. The lighter muds have a higher carbonate and sand content, the darker muds are clay-rich, and their interbedding is inferred to represent the settlement of seasonal flood plumes (dark grey) against a background of more general hemipelagic mud (light grey). This bedded-mud facies is clay-rich (see Fig. 6a–c), mainly restricted to cold climate parts of Unit A (when the shoreline was nearby), and does not occur within the underlying Canterbury Drifts. (**b**–**f**) composite FMS resistivity images of selected drift intervals; white and yellow–gold indicate high resistivity (concretionary layers, sands); orange to brown, lower resistivity (sandy silts, silts); black, borehole washout. The variety of style in the *c*. 30–110 cm thick sand beds should be noted; some are both sharp-based (**c**, 171.9 mbsf; **d**, 255.8 mbsf) and sharp-topped (**b**, 113.5 mbsf), others are gradationally based (**b**, 113.8 mbsf; **d**, 259.9 mbsf) and gradationally topped (**c**, 171.4 mbsf; **e**, 317 mbsf). In the more deeply buried drifts, incipient cementation may give rise to high resistivity in sand-bed cores (arrowed; **e**, 317.3, 318.1 mbsf). The sands are set in a background of pervasively interlaminated, laterally pinching and swelling, silty sand (lighter) and sandy silt (darker) on scales of *c*. 1–10 cm. Some intervals of background mud are sand-rich (e.g. **b**, 113–115 mbsf), others mud-rich (e.g. **c**, 167–172 mbsf). The absence of discrete, thicker sand beds from drift Unit C (**f**, 431–434 mbsf), but retention of the thin-bedded, current-drift fabric in the silty sands and sandy silts, should also be noted.

burrowed or bioturbated, and punctuated by 2–300 cm thick beds of muddy, very fine-grained quartzofeldspathic sand. Internally, some of the thicker sand units display pulsatory changes in sand or mud content; organized Bouma turbidite structures (see Stow *et al.* 1998) are not present. Some sands have both gradational bottoms and tops, and comprise a reverse- to normal-graded mud–sand–mud triplet similar to descriptions of other sediment drift deposits (Stoker *et al.* 1998) and to the idealized drift facies model of Faugères *et al.* (1984) and Stow *et al.* (1998). The overall characteristics of the Site 1119 muds, silts and sands below 86 mcd coincide with those first

described for sediment drifts from the Feni Drift by Faugères *et al.* (1984), namely, 'contacts between the different facies may be more or less planar and sharp, distinctly erosional, or completely gradational, and all three types are equally common at the base or at the top of separate beds ... Mottling occurs throughout ... together with other more or less distinct and isolated pockets and streaks.' Virtually all of the cored sediments of the Canterbury Drifts, between 86 and 514 mcd (TD at Site 1119), therefore, belong to the 'silt and sand' and 'mottled silt and mud' sediment drift facies of Faugères *et al.* (1984) and Stow *et al.* (1998).

Finally, the 328 m drilled thickness of Units B and C at Site 1119 appears to contain only two thin (<1 cm thick) beds of graded sand that might be interpreted as slope turbidites (Carter *et al.* 1999). Overall, therefore, the lithology of the dominantly siltstone and mudstone sediment pile (which is best revealed by FMS images; Fig. 4) is consistent with the seismic geometry of the deposits (see Fig. 3a) and with contourite deposition from systematically fluctuating bottom currents.

Grain-size textural distributions

Grain-size distributions have been grouped according to stratigraphic unit, in order downwards from the sea bed (Table 1). Samples from units A and B are similar in their lithological range, comprising a background of silty mudstone–muddy or sandy siltstone with distinct modes of very fine (<5 μm), fine (8–16 μm) and coarse (35–60 μm) silt, and interspersed beds of muddy, very fine- or medium-grained sandstone (modes 100–130 and 235–440 μm) (Figs 5a–f and 6b,c). Unit C (large drift D11) differs in its lack of sand interbeds and in having a dominant coarse, rather than very fine or fine, silt mode (Figs 5g and 6a). For graphical presentation, samples have been divided into two main facies groups, silty mudstone + muddy siltstone and silty sandstone + sandy siltstone, respectively. Generally, these groups share common modes though with different proportions of each, as represented by average cM:sZ:sS ratios of 45:47:9 and 14:24:63 for the mudstone and sandstone facies, respectively (Table 1).

Sediments of grain sizes 12, 35 and 110 μm diameter become entrained at current speeds of *c*. 11, *c*. 15 and *c*. 25 cm s^{-1}, respectively (Miller *et al.* 1977; McCave *et al.* 1996; McCave 2005; Table 1). Against such a background, the sands that occur interspersed throughout the Unit B drifts commonly display medium to coarse sand modes (235–440 μm), indicative of enhanced current strengths up to 50 cm s^{-1}. That some sand beds have sharp bases indicates that in such cases even stronger currents eroded the underlying muddy sea bed prior to waning to allow sand deposition.

Depth plots of sediment texture

Despite a variable sample spacing (Fig. 7a) and core gaps (Fig. 3), depth-ordered, contiguous-sample plots of the cM:sZ:sS ratio and mean and modal grain sizes reveal useful information about grain-size trends against stratigraphic height (Fig. 7b and c).

The succession is punctuated by episodic sand beds, which occur within a silt- and cohesive mud-dominated sediment background. A long-term trend of increasing cohesive mud and decreasing sand and silt starts at *c*. 390 mcd (*c*. 2.75 Ma). This trend passes up across the downlap unconformity and into the clinoform downlapping sediments of unit A, where cM:sZ:sS ratios as mud-rich as 54:40:7 occur. Although a single trend line can be fitted to this long-term mud increase, the data could also be interpreted as showing stepped increases in mud content at *c*. 350 mcd (2.3 Ma) and *c*. 150 mcd (0.7 Ma).

Above 320 mcd (unit B4 and above; small drifts), sand is mostly represented by terrigenous grains, dominantly quartz; between 320 and 440 m (unit B5; drift tails), sands also contain large numbers of calcareous microfossils and shell fragments (Carter *et al.* 1999). The background silts and muds of drift units B1–B5 have average cM:sZ:sS ratios of 41:50:9, in comparison with 21:52:28 for unit C (large drift D11). In parallel with the trend of increasing mud content upwards, the dominant grain-size mode decreases from coarse silt (40–55 μm) in unit C, to fine silt (9–16 μm) in units B4–A2, to very fine silt (<5 μm) in unit A1 (Table 1). The two dominant mean sand grain sizes, similar across the succession, are very fine (100–130 μm) and medium (250–440 μm) sand, with a concentration of the latter, coarser mode in small drifts B3 and B4 (Fig. 7c, Table 1).

Canterbury Drifts onland (Bluecliffs Silt Formation)

A nearly complete sequence through the Bluecliffs Silt Formation occurs at its type locality in the Otaio River, a little inland from Timaru, central South Island (Figs 1b and 8). Samples were collected at Otaio River through the middle part of the formation (*c*. 50–320 m above the base), above its poorly outcropping basal part. Samples were also collected from two other well-exposed sections through Bluecliffs Formation (Te Ngawai River; central basin, inland of Otaio River, Fig. 8b; south branch of Waipara River; northern

Table 1. *Summary table of grain-size modes for the Canterbury Drifts at Site 1119 and onland exposures of the Bluecliffs Formation*

		ODP Site 1119 (all samples)													
		Cohesive	Sortable Silt	Sand	*n*	%'mud'	%'sand'	S:M							
< 20% sand	M	44.74	46.73	8.54	115	91.46	8.54	0.09							
20–50% sand	mS	24.71	40.97	34.32	50	65.68	34.32	0.52							
> 50% sand	S	13.75	23.53	62.72	38	37.28	62.72	1.68							
Drift 11	zC	20.61	51.68	27.72	17	72.28	27.72	0.38							
		ODP Site 1119 (mudstone facies only)							Modal Grain Diameters						
		Cohesive	Sortable Silt	Sand	*n*	%'mud'	%'sand'	S:M	vfz	1st fz	2nd mz	3rd cz	4th vfs	fs	ms–cs
	Unit A1	46.39	45.99	7.62	29	92.38	7.62	0.08	<5	8–16		40–50	100–117		or 350
	Unit A2	42.83	49.64	7.53	21	92.47	7.53	0.08	<5	9–13		37–42	100–130		or 300–355
	Unit B1	31.44	55.58	13	5	87.02	13	0.15	<5	11–13		35–50	100–110		or 350
	Unit B2	33.48	51.09	15.42	29	84.57	15.42	0.18	<5	10–13		35–50	100–130		or 285–440
	Unit B3	27.8	37.99	34.2	11	65.8	34.2	0.52	<5	9–16		35–65	110–125	or 180–275	or 265–330
	Unit B4	25.21	40.45	34.33	13	65.66	34.33	0.52	<5	12–16		35–60			235–405
	Unit B5	22.34	43.22	34.43	8	65.56	34.43	0.53	<5		16–28	or 35–55		125–270	
	Unit C	55.07	8.91	0.12	17	63.97	0.12	0	<5			40–55		170–260	
	All (except C)	32.79	46.28	20.93	116	69.18	18.32	0.26							
	All (including C)	35.57	41.61	18.33	133	77.18	18.33	0.24							
				Total samples	133										
Bluecliffs Silt onland															
Walpara River	All samples	12.66	46.4	40.94	20	59.06	40.94	0.69	<10		27	or 55–65	or 80–140		
Te Ngawai River	All samples	7.96	41.12	50.92	36	49.08	50.92	1.04	<10				80–105		700–1200
Shag River mouth	All samples	7.45	45.96	46.59	16	53.4	46.59	0.87	<10			45–50	or 80–105		300–800
Otaio River	All samples	5.67	46.94	47.39	36	52.61	47.39	0.9							
	Silt facies	6.97	51.62	41.42	17	58.58	41.42	0.71	<10				70–100		300–800
	Sand facies	4.51	42.75	52.74	19	47.26	52.74	1.12	<10				70–100		720–960
	All onland	8.43	45.1	46.46	108	53.54	46.46	0.87							
Grain diameter (μm)									<10	12	30	60	110	250	450
Entrainment velocities (cm s^{-1})									cohesive	11	13	17	25	38	50

Inferred current speed figures are estimated for 1 m above the bed, based upon Miller et al. (1977) and McCave et al. (1995).

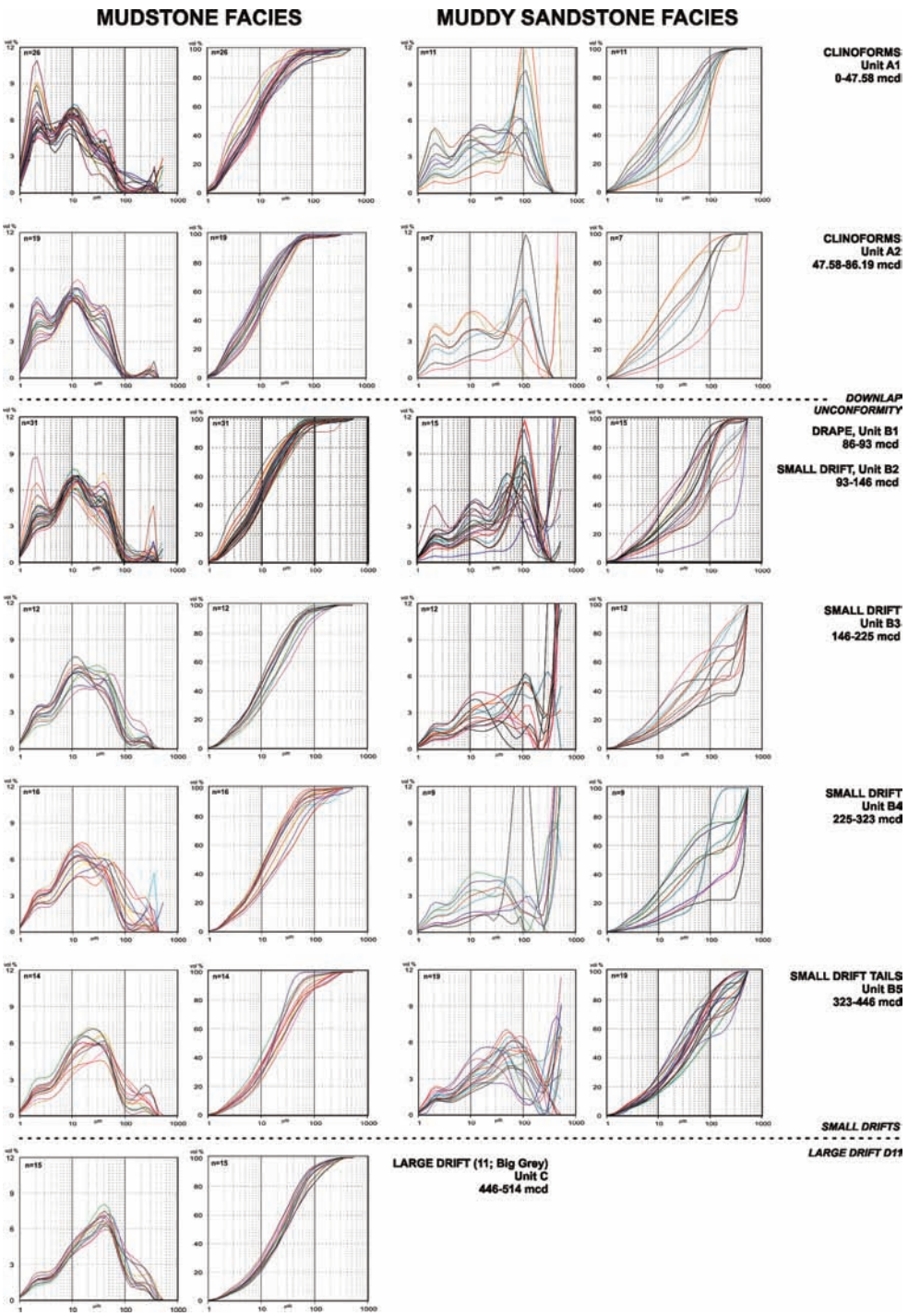

Fig. 5. Grain-size distributions for ODP Site 1119 sediments, determined using a Malvern laser particle sizer fitted with a 1.2–600 μm lens. Left column graph-pair and right column graph-pair comprise histogram and cumulative frequency plots for the mudstone and muddy sandstone facies from each specified stratigraphic interval, respectively. Data plotted on a logarithmic *x*-axis for all graphs; *y*-axes indicate volume percentage and cumulative volume percentage, respectively.

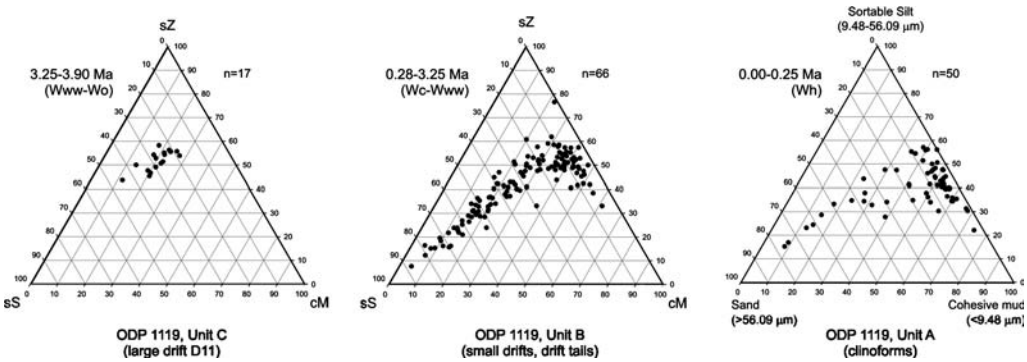

Fig. 6. Tri-plots for cohesive mud:sortable silt:sortable sand (sS) (cM:sZ:sS) for sediments from units A, B and C at Site 1119.

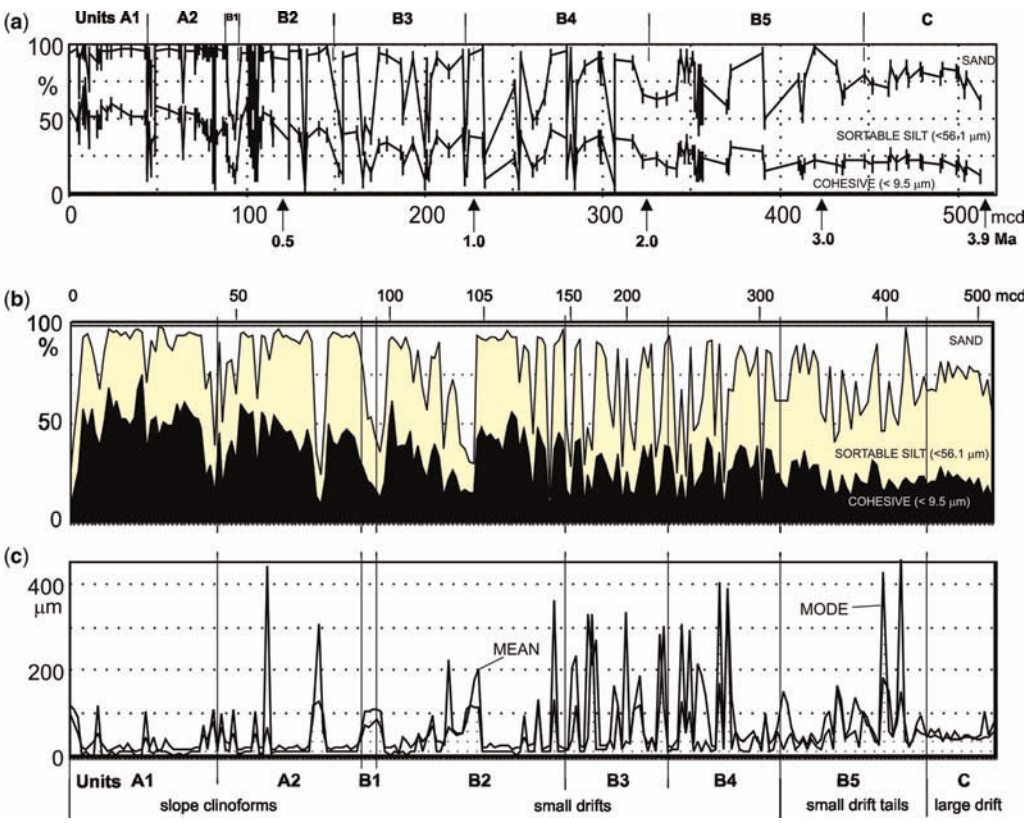

Fig. 7. (**a**) Sediment textural data for ODP Site 1119 plotted against metres composite depth, and (**b**) collapsed depth (i.e. samples plotted left to right in depth order and contiguous to each adjacent sample, regardless of the true interval that separates them). Percentage amounts of cohesive mud (black in **b**), sortable silt and sortable sand are plotted throughout Site 1119. (**c**) Grain-size mean and primary mode against collapsed depth (note the correspondence in pattern between these two measures, and the correlation of coarser peaks with the sand-rich intervals delineated in (**a**) and (**b**)).

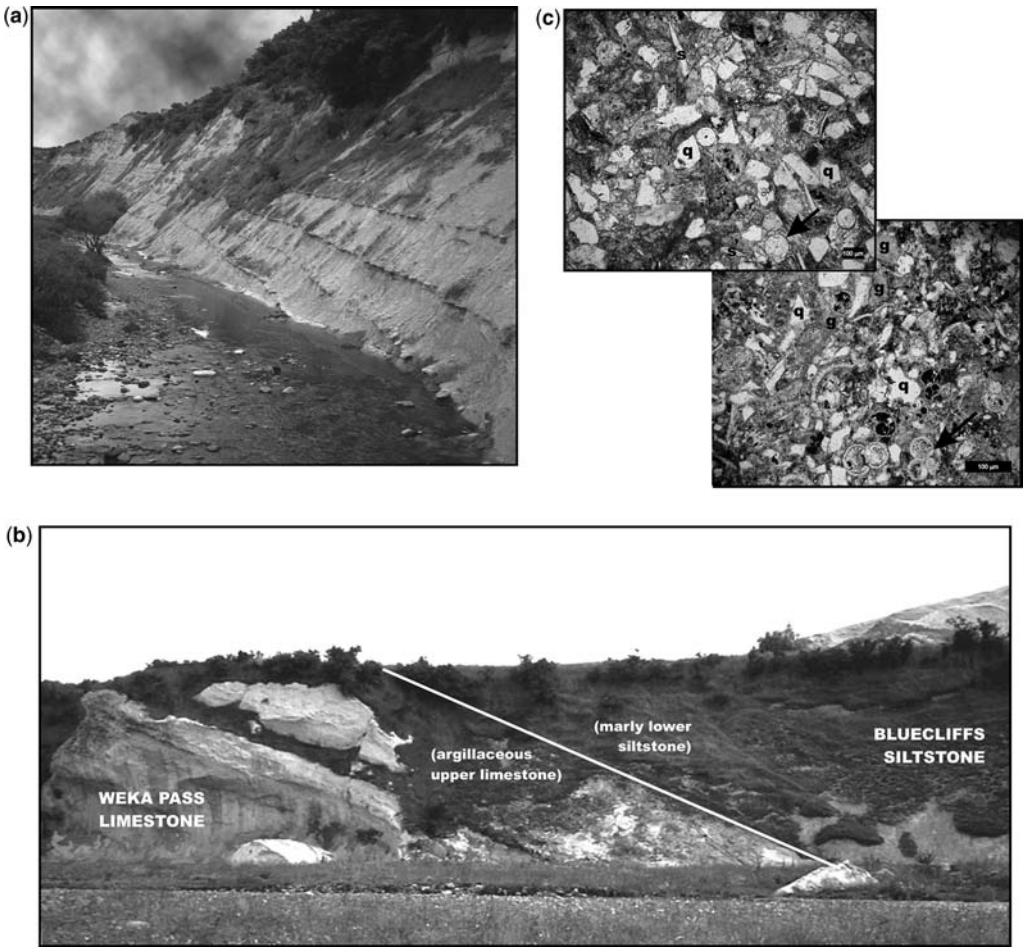

Fig. 8. (**a**) Type section of Bluecliffs Formation, Otaio River, South Canterbury, beds dipping 20° ESE. (Note the *c*. 20 cm thick cemented layers located about 3 m apart, which lie at and just above intervals of sand, some sharp-based and normally graded, others gradationally based with reverse-to-normal grading.) (**b**) Outcrop transition between Weka Pass Limestone and Bluecliffs Formation Siltstone, Te Ngawai River, South Canterbury. The gradational change between the two units, indicated by the argillaceous upper limestone and marly lower siltstone intervals, should be noted. (**c**) Photomicrographs (×80, plane-polarized light) of (above) Goodwood Limestone, Shag River Coast and (below) Bluecliffs Formation, Te Ngawai River, basal marly siltstone. The poorly sorted nature should be noted; clayey matrix contains silt-sized grains of clear, angular quartz (q), sericite (s), pelleted glauconite (g), sponge spicules (arrowed, upper photograph) and planktic foraminifers (arrowed, lower photograph). Scale bars represent 100 μm.

basin), and through a coastal outcrop of the upper part of the formation on the coast south of Shag River ('Goodwood limestone'; southern basin).

Stratigraphy and lithology

The *Otaio River section* is the type for both the Bluecliffs Formation and the local New Zealand Early Miocene Otaian biostratigraphic stage (23.2–21.7 Ma), and because of this has recently been subjected to detailed study (Morgans *et al.* 1999). The section comprises a *c*. 330 m thick succession of regressive, terrigenous siltstone and sandstone, marly in its lower part, which succeeds an offshore carbonate platform deposit (Weka Pass Limestone; *c*. 30 m thick) and is followed by a shoaling shelf to shoreface, sand-dominated unit (Southburn Sand; 150+m thick). The section represents the eastward passage of the slope–shelf succession, as it built eastwards and downlapped onto the pre-existing, quasi-horizontal, regional Oligocene carbonate platform (Fig. 2a). That the

succession in Otaio River is only *c*. 330 m thick, compared with *c*. 2000 m thick for its equivalent beneath the modern outer shelf and slope, is consistent with its accumulation in a relatively nearshore geographical position in initial platform water depths of perhaps 450–750 m.

Bluecliffs Silt comprises a background continuum of sandy siltstone–silty very fine sandstone, punctuated by 1–5 m spaced beds or intervals of muddy, medium- to coarse-grained sandstone up to 30 cm thick (Figs 8a and 9b). The sand beds are often concretionary, and sometimes glauconitic or contain *in situ* bivalved venerids. Some sandstone beds are sharp-based and grade up into overlying siltstone, others are double-graded against both underlying and overlying siltstone. Small-scale bioturbation, often marked by pyritized burrows, is pervasive, but not to a degree that homogenizes the thicker sand–silt rhythmicity. Rare hydroplastic deformation in some beds attests to a sea-floor slope. Fossils include scattered molluscs (*Limopsis, Zeacolpus, Stiracolpus, Palomelon, Dentalium*), shell fragments, annelids and solitary corals (*Flabellum, Notocyathus*), all of bathyal aspect, and abundant microfossils and nannofossils. In their detailed study of the Otaio River section, Morgans *et al.* (1999) showed that sediment cyclicity occurs as *c*. 5 m spaced peaks in foraminiferal abundance which co-vary with decreases in coarse sediment (>74 μm) content. Planktic taxa make up 45–85% of total Foraminifera, and nannofossils up to *c*. 50% of the sediment matrix. Foraminiferal census counts suggest deposition of the lower part of the section at *c*. 600 m water depth, shoaling to depths of *c*. 100 m in the upper part, where the molluscan fauna becomes more diverse and contains taxa of uppermost bathyal to outer shelf aspect. The composition of nannofossil and foraminiferal assemblages indicates deposition from a cool-temperate water mass that was eutrophic, vertically well mixed and located in the transition zone between coastal and fully oceanic water.

The above description of Bluecliffs Silt at its type locality, and inferences therefrom, applies with only minor local modification to other outcrops of Bluecliffs Formation throughout the basin.

In the south branch of the Waipara River (Fig. 1b), the formation is 300 m thick and again early Miocene (Otaian) in age. The basal few metres (Pahau Siltstone of Andrews 1963) are calcareous and mildly glauconitic, marking the transition from the underlying carbonate platform deposit (Weka Pass Limestone). A conspicuous interval of well-sorted sands occurs between *c*. 50 and 100 m above the base (the Crantara Sandstone of Andrews 1963), above which again the formation becomes sandier upwards towards the shoreface sands of the overlying Southburn Sand (=Mt. Brown Beds). The Crantara Sandstone contains about six sharp-based, 1–3 m thick units of massive sand, which grade up to siltier intervals of either bioturbated sandy silt or centimetre-scale sand–silt flaser and lenticular bedding. These facies are clearly both rhythmic and strongly bottom-current influenced.

At *Te Ngawai River* (Fig. 1b), the Bluecliffs Silt is 324 m thick (Douglas 1975), with a slightly calcareous base that is transitional from the underlying limestone. Foraminifera indicate an age of either latest Oligocene (Waitakian Stage, *c*. 22.7–25.2 Ma; Finlay 1953) or earliest Miocene (Otaian Stage, *c*. 19.0–22.7 Ma; Vella, *in* Eade & Kennett 1962). Well-washed outcrops display an indistinct, 1.5–5 m spaced, rhythmicity of 20–40 cm thick slightly sandier layers separated by less sandy siltstone. The formation is bioturbated and slightly glauconitic throughout (Fig. 8c). The upper 15 m of the formation (separated by Douglas (1975) as the Upper Member) is sandier, more glauconitic, more fossiliferous and more bioturbated as it approaches the contact with the overlying shallow shelf–shoreface Southburn Sand. In his detailed study, Douglas (1975) showed that (1) the ratio of planktic:benthic Foraminifera is highest (between 60:40 and 75:25) in the lowest 30 m of the formation, averages 55:45 between 30 and 290 m, and falls to 20:80 over the top 35 m, and (2) between 5 and 30% of the sediment is a non-terrigenous coarse fraction, comprising foraminifers, molluscan shell fragments and glauconite. These characteristics are closely similar to those described by Morgans *et al.* (1999) for the Bluecliffs Silt at Otaio River, and indicate again that the formation represents shoaling (*c*. 600–100 m palaeodepth) oceanic slope environments adjacent to a narrow, sandy shelf–shoreface system to the west.

At the southern end of the Canterbury Basin, the early Neogene terrigenous succession is unusually sandy, cropping out around Dunedin as the muddy Caversham Sandstone (Bishop & Turnbull 1996). A similar facies occurs also offshore in exploration well Endeavour-1, off Oamaru. North of Dunedin, on the coast south of the Shag River mouth (Fig. 1b), the upper part of the Caversham Sandstone interval is represented by rhythmically bedded, Bluecliffs-facies bioturbated silts and muddy sands, 10–20 m thick packets of which show lensing, lateral onlap and other evidence of current-influenced deposition (Carter, R., *et al.* 1996, fig. 7b). The 20–40 cm thick muddy sandstone beds at the base of individual sedimentation units, which sometimes contain abundant siliceous sponge spicules (Fig. 8c) and diatom frustrules, often carry a concretionary calcite cement, causing the rather misleading name Goodwood

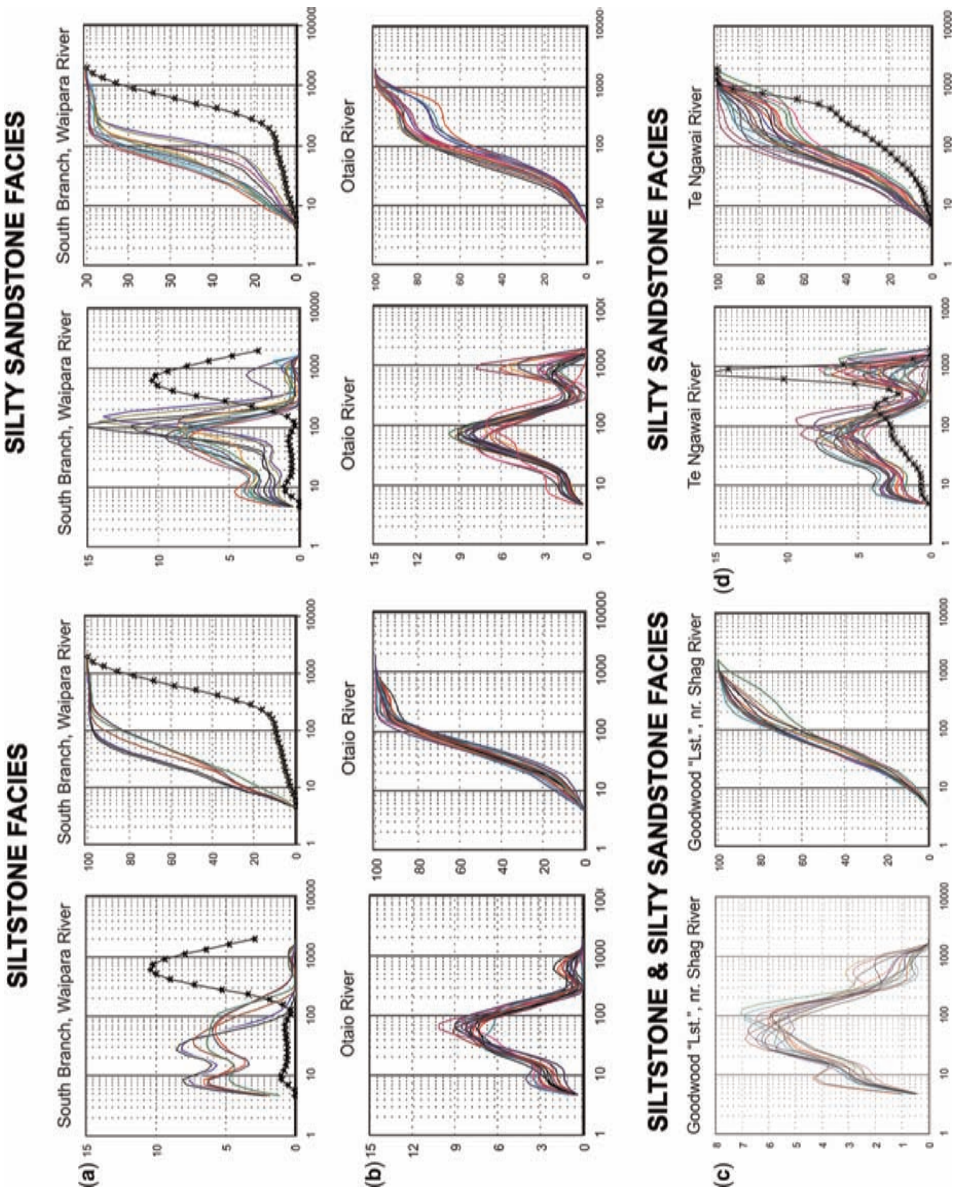

Fig. 9. Grain-size distributions for the onland Bluecliffs Formation from: (**a**) South Branch, Waipara River; (**b**) Otaio River; (**c**) coast near Shag River mouth; (**d**) Te Ngawai River. Determined using a Malvern laser particle sizer fitted with a 4–2000 μm lens. Left column graph-pair and right column graph-pair for (**a**) and (**b**) comprise histogram and cumulative frequency plots for the siltstone and sandstone facies from each locality, respectively. (**c**) and (**d**) are similar, but samples are not subdivided into silt and sand facies at each locality. Data plotted on a logarithmic *x*-axis for all graphs; *y*-axes indicate volume percentage and cumulative volume percentage, respectively.

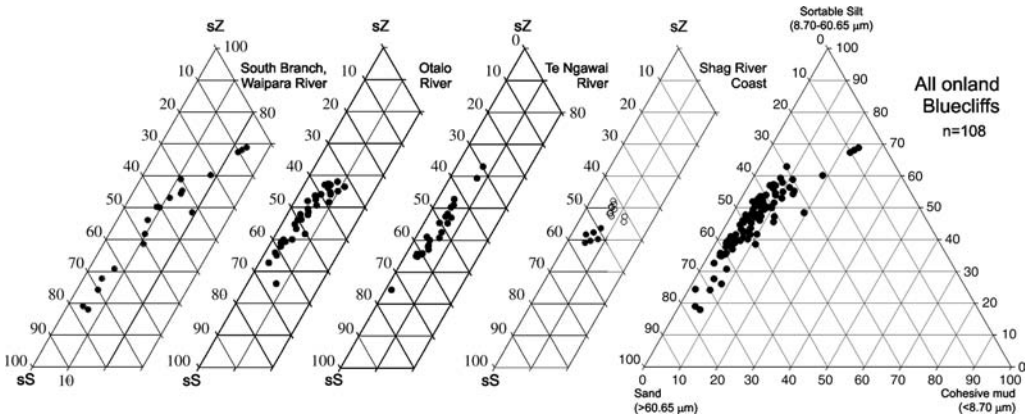

Fig. 10. Tri-plots for cohesive mud:sortable silt:sortable sand (sS) (cM:sZ:sS) for the onland Canterbury Drifts at (left to right): South Branch, Waipara River, Otaio River, Te Ngawai River, and coast south of Shag River mouth. Samples are replotted as a single, composite set on the full triangle (right).

Limestone (Service 1934) to be assigned to them. The 'limestone' succession is of early Miocene age (Otaian to Altonian Stages; *c*. 16–23 Ma; Benson, *in* Fleming 1955).

Grain-size textural distributions

Bluecliffs Formation sediments from all the onland Early Miocene localities are closely similar in their sedimentary characteristics and grain-size texture. They comprise a continuum of moderately sorted, silty sands and sandy silts with three dominant modes of very fine silt (<10 μm), very fine sand (70–105 μm) and medium–coarse sand (300–800 μm) (Figs 9 and 10; Table 1). As at Site 1119, the grain-size modes are common to both the sandy and silty facies, but differ almost symmetrically between facies in their relative proportions. For instance, at Otaio River, sands and silts have cM:sZ:sS ratios of 5:43:53 and 7:52:42, respectively, compared with a ratio of 8:45:46 for the average of all 108 onland samples (Table 1). The great majority of samples contain <12% mud, apart from four samples from the Pahau member at the base of the Bluecliffs Formation at Waipara River, which have mud contents of 18–23%.

Depth plots of sediment texture

Depth-ordered, contiguous-sample plots of the cM:sZ:sS ratio and mean and modal grain sizes demonstrate the stratigraphic and regional homogeneity of the Bluecliffs Formation, and reveal useful information about grain-size trends (Fig. 11).

The lower *c*. 50 m of the formation at Waipara and Te Ngawai is noticeably richer in mud (Fig. 11a and b), and all sections are characterized by decametre-wavelength cycles of fluctuating sZ:sS ratio, which are often paralleled by changes in the mean and modal grain size. The main sediment mode increases in size upwards through the basal parts of the Waipara River and Te Ngawai sections and thereafter fluctuates slightly in sympathy with the changing mean grain size. At Otaio River (section between 50 and 220 m) the very fine sand mode (70–100 μm) remains remarkably constant throughout fluctuations in mean grain size, which represent the intermittent presence of the medium sand mode.

Comparison between offshore and onshore drifts

The offshore Plio-Pleistocene strata from Site 1119 and the onshore, Late Oligocene and younger Bluecliffs Formation belong to the same stratigraphic body, which is the prograding prism of upper slope sediment that I have termed the Canterbury Drifts (Fig. 2).

The average compositions of sediment samples from different stratigraphic levels are plotted on a cM:sZ:sS textural diagram in Figure 12, which summarizes the same dataset that is plotted as individual points in Figures 6 and 10. A striking pattern emerges. Early Miocene sediments are low in cohesive mud, and form a tight-knit cluster of sandy silts and silty sands. In contrast, samples from mid-Pliocene drift, Unit C, contain on average *c*. 15% less sand and *c*. 15% more cohesive mud than the onland Bluecliffs Formation, and are intermediate between the Early Miocene samples and Late Pliocene–Pleistocene samples from Unit B5 at Site 1119. Successively younger Site 1119 intervals,

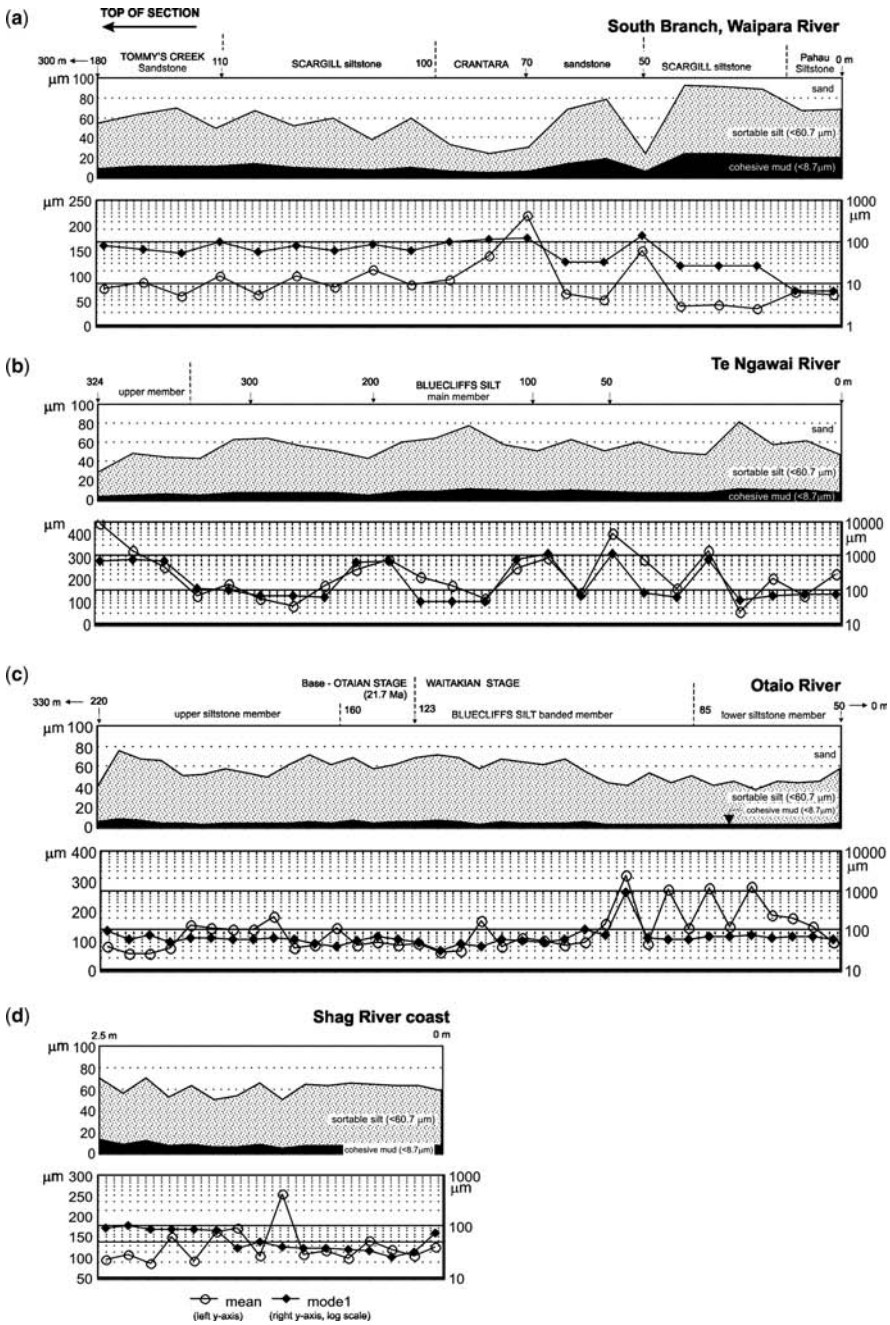

Fig. 11. Sediment textural data for onland Bluecliffs Formation localities plotted against collapsed depth (i.e. samples plotted left to right in depth order and contiguous to each adjacent sample, regardless of the true interval that separates them). Upper graph of each pair plots percentages of cohesive mud (cM; black), sortable silt (sZ; shaded) and sortable sand (sS; white); lower graphs plot the mean (left-axis arithmetic scale) and modal (right-axis logarithmic scale) grain size. (**a**) South Branch, Waipara River; lower and middle parts of Bluecliffs Formation (0–180 m of the total 300 m); (**b**) Te Ngawai River; complete section through Bluecliffs Formation (0–324 m); (**c**) Otaio River; middle parts of Bluecliffs Formation (50–220 m of the total 330 m); (**d**) coast south of Shag River mouth; small, characteristic interval of Bluecliffs Formation (3.5 m thickness).

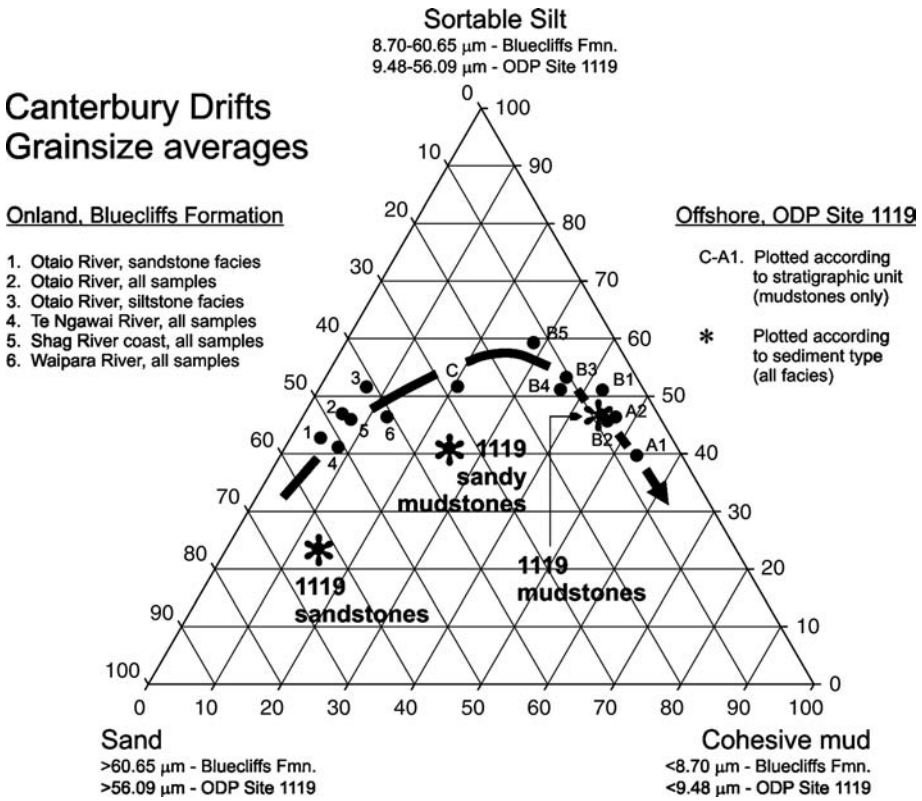

Fig. 12. Tri-plot for values of cohesive mud:sortable silt:sortable sand (sS) (cM:sZ:sS) for Canterbury Drift sediments from both offshore (ODP Site 1119) and onshore (Bluecliffs Formation). The average value is plotted for sediments from each locality (see Fig. 10) or indicated stratigraphic interval (see Fig. 6), and also for the three commonest facies variants at Site 1119, namely sandstone, sandy mudstones and mudstone.

B4 to B1, lie along a path of increasing cohesive mud, which is 5% higher than Unit C in Unit B5 and increases to 25% higher in the topmost drift, Unit B2. The trend to higher mud continues through into the clinoform Unit A, with Unit A1 samples containing 20% less sand and 33% more cohesive mud than Unit C samples.

Synthesis

The previous part of this paper contains a synopsis of the regional nature of the Late Oligocene to Recent Canterbury Drifts, and presents new data to help delineate their character. This information, in turn, points to new oceanographic, climate-history and stratigraphic perspectives, as discussed below.

Time period of drift deposition

The accumulation of substantial sediment drifts requires an extended period of stability, both geological (controlling, via tectonics, the source of sediment, the transport pathway and the site of deposition) and oceanographic (controlling, via current flows, the mechanism of deposition).

Morgans *et al.* (1999) showed that the base of the Early Miocene Otaian stage lies at 73 m above the base of the Bluecliffs Formation as exposed at Otaio River, and estimated its age as 21.7 Ma. A further *c*. 50 m of poorly outcropping calcareous siltstone (Waitoura Marl, here treated as a basal member of Bluecliffs Formation) lies beneath this section and above the top of the Weka Pass Limestone, indicating that the incoming of post-limestone terrigenous sediment, and the true base of the Bluecliffs Formation, lies *c*. 123 m below the base-Otaian boundary. Assuming a sedimentation rate of 10 cm ka^{-1}, this thickness of sediment corresponds to 1.23 Ma, which yields an age estimate of 22.93 Ma for the local base of the Bluecliffs Formation. Thus at Otaio River terrigenous sediment first appeared in the Early Miocene, about 0.87 Ma later than the 23.80 Ma Oligocene–Miocene boundary.

The eastward progradational nature of the Bluecliffs Formation implies that successions along the western edge of the Canterbury Basin will be both thinner and older at their base than is the section at Otaio River. Consistent with this inference, some earlier workers inferred an age of Waitakian (25.2–22.7 Ma) for outcrops of Bluecliffs Formation at Te Ngawai River (see Fig. 1). The earliest Bluecliffs Formation onland, and the start of regional terrigenous drift sedimentation in eastern New Zealand, therefore, dates from *c*. 24 Ma in the Late Oligocene. Because the Canterbury Drifts everywhere overlie older, *c*. 28–24 Ma, greensand–carbonate platform drifts of the Kekenodon Group, it is clear that the *c*. 24 Ma date corresponds not to the start of drift sedimentation *per se*, but rather to the start of supply of terrigenous sediment from the western plate boundary. The almost simultaneous appearance of terrigenous sediment at *c*. 24.0 Ma in offshore abyssal drifts of ENZOSS (ODP Site 1124; Joseph *et al.* 2004) and terrigenous turbidites of similar age in the Waiau Basin (Carter *et al.* 2005) confirms the Late Oligocene–Early Miocene appearance of a new, voluminous and widespread source.

In summary, the terrigenous Canterbury Drifts have a longevity of *c*. 24 Ma. This results from their deposition along a passive continental margin, which, over that period of time was (1) tectonically stable, and (2) consistently fed with sediment from a nearby, uplifting plate boundary.

Transport pathways for drift-feeding sediment

Since the Late Oligocene, terrigenous sediment has been eroded from mountains aligned along the western South Island plate boundary and delivered by east-flowing rivers to the coast. The mechanism whereby this terrigenous sediment was then moved across the shelf and onto the upper slope is less clear.

Along eastern South Island today, modern terrigenous sand is restricted to the shoreface and inner shelf, and the middle and outer shelf are either mud-covered (Herzer 1981) or, under the influence of the Southland Current, comprise shelly and bryozoan-rich facies (Carter *et al.* 1985). Although storm-engendered, cross-shelf mud-hopping is a feasible mechanism for the delivery of clay and very fine silt to the slope, it is much less likely for medium- to coarse-grained sand grain sizes. How, then, has such sand been delivered to the Canterbury Drifts in the past, and how does it cross the shelf today? There are at least three possible answers to these questions.

First, the width of the early Neogene shelf was much less than it is today (e.g. Fulthorpe & Carter 1991, fig. 4b), making direct cross-shelf sand transport more feasible. *Second*, since about 3.1 Ma, and to a lesser extent before, eustatic sea-level falls of up to 130 m during cold or glacial periods have intermittently narrowed the shelf by exposing its inner portion and moving the shoreline seaward up to many tens of kilometres, which again would have enhanced the chance of cross-shelf sand transport and deposition around the shelf-edge (Carter *et al.* 2004*b*). *Third*, in the southern part of the basin the slope and shelf-edge are dissected by numerous submarine channels and canyons (Krause 1966; Herzer 1979) around the headward part of the Bounty Trough. Turbidity currents travelling down these canyons and into the Bounty Channel system are deflected left by the Coriolis effect, resulting in preferential overspilling on the left (north) bank (Carter & Carter 1988) and the delivery of abundant terrigenous sediment along the north-flowing paths of both intermediate AAIW and abyssal CDW. Although similar ancient (buried) canyon systems are rarely imaged on seismic profiles through the offshore basin, they do occur (e.g. Herzer & Lewis 1979; Lu & Fulthorpe 2004).

In summary, the bulk of the sediment that now comprises the Canterbury Drifts was probably transported to the continental slope through shelf-edge indenting canyons, aided by the direct dumping of shoreface sediments around the shelf-edge and canyon heads during sea-level lowstands.

Sedimentary structures accompanying drift deposition

In outcrop, the Bluecliffs Silt comprises mildly bioturbated, poorly bedded terrigenous siltstone and very fine sandstone, punctuated by beds of very fine or medium- to coarse-grained muddy sand, sometimes concretionary. Sedimentary structures are usually not conspicuous. However, data from ODP Site 1119 reveal the presence of abundant sedimentary structures in the Canterbury Drifts, most of which are also present in outcrop.

The offshore Canterbury Drifts are dominated by alternating plane-beds of sandy and muddy silt on a centimetre scale, with interspersed muddy sands up to several metres thick; millimetre-scale planar and undulose lamination occurs within some thicker sand beds. Cut-core and outcrop surfaces generally present as unstructured, massive, bioturbated muddy silt, sandy silt and silty sand, occasionally with subtle centimetre-scale layering of slightly different colours or grain sizes. Given the visual rarity of strong macroscopic layering in core and outcrop, it is surprising that FMS images of the borehole wall show the pervasive presence

throughout the Site 1119 drillhole of resistivity layering at the centimetre-scale (Fig. 4). This layering reflects the presence of interbedded muddy and sandy silts, is often slightly undulose, consistent with the presence of ripple-like features, and is only mildly disturbed by bioturbation.

Thicker sand beds, up to 3 m, may have either sharp or gradational bases and tops. Most commonly, these beds are either normally graded with sharp, erosive bases against underlying siltstone, or are doubly graded, with a reverse-graded base and a normally graded top. Given sand grain sizes between 80 and *c*. 1000 μm, this implies (1) currents that are strong and then gradually wane, or that gradually increase and then gradually wane, respectively, and (2) current velocities in the range of 20–70 cm s^{-1} (Table 1).

The Canterbury Drifts were deposited from strong bottom currents that waxed and waned episodically at Milankovitch periodicity to deposit the thicker sand units (Carter *et al.* 2004*a*), and gentler currents (5–15 cm s^{-1}) that operated regularly at short periodicity to produce the pervasive, centimetre-scale, mud–silt, background layering.

In summary, both offshore and onland, the Canterbury Drifts contain a range of sedimentary structures indicative of contourite deposition. Where not homogenized by bioturbation, these structures include pervasive centimetre-scale interbeds of background muddy and sandy silt, in which occur interspersed thicker, sharp-based normally graded, and gradationally based double-graded sandstones.

Oceanographic and climatic controls on drift deposition

Deposition of a large sediment drift requires the stable operation of a significant geostrophic current over an extended period of time. Such major ocean currents represent flow responses to the particular configuration of an ocean basin. Changes to basin configuration of sufficient magnitude to reset geostrophic flows generally take place over periods of tens of millions of years or longer, unless rapid gateway opening or shutting occurs.

In the modern ocean, deep, cold water flows generated at high southern latitudes pass east of New Zealand to flow northward into the Pacific basin. The three main flows are: circumpolar deep water (2000–4500 m; generated by sinking waters around the periphery of Antarctica; Carter & McCave 1997); AAIW (800–1100 m; generated by subduction at the Antarctic Polar Front (APF); Lynch–Stieglitz *et al.* 1994); and SAMW (300–800 m; generated by subduction at the Subantarctic Front; Morris *et al.* 2001). Predecessor flows to these date back to the inception of the 'modern' stratified ocean at *c*. 33.5 Ma, when the Southern Ocean was created by the deep-water separation of Tasmania and Antarctica (Exon *et al.* 2001). Cold water flows of Southern Ocean derivation have therefore affected the deposition of the Canterbury Drifts throughout their 24 Ma history. Near Site 1119 the shallowest of the modern flows, SAMW, is augmented by an outer shelf–upper slope current jet (Southland Current; Heath 1972; Chiswell 1996; Sutton 2003), which follows the NE-oriented, margin-parallel path of the Subtropical Front off eastern South Island (Sutton 2003).

At 394 m water depth, Site 1119 lies a little seawards of the Southland Current core and at the top of the zone of north-flowing SAMW (Morris *et al.* 2001). Deeper still, at around 800 m water depth, SAMW is underlain by similarly north-flowing AAIW. In consequence, the upper clinoform and small-drift parts of Site 1119 were deposited from SAMW, whereas the basal *c*. 100 m of the core (big drift 11) was probably deposited under AAIW (Carter *et al.* 2004*a*) (Fig. 3b). The change in drift architecture observed in seismic profiles at *c*. 3.1 Ma may have resulted from the initiation then of the SAF, or the movement of the STF into its present postion, or both, the latter accompanied by SAMW generation and Southland Current flow. Alternatively, should both these fronts have already existed in approximately their modern positions, the change from large AAIW drifts to small SAMW drifts may simply reflect shoaling and accretion of the sea bed from AAIW to SAMW depths.

Similarly, the change in the Canterbury Drifts from simple slope clinoforms to clinoforms with large drifts at *c*. 15 Ma (Lu *et al.* 2003) is also likely to mark a significant shift in the dynamics of the northward along-slope current regime. Corresponding as it does to the worldwide Late Miocene cooling caused by growth of the East Antarctic ice sheet, this change from clinoform to large drifts may mark the inception of the APF and the first generation of steady AAIW circulation.

In summary, the Canterbury Drifts were deposited from persistent, north-directed, cold-water, intermediate-depth, geostrophic currents. Changes in their internal geometry, from clinoform to large to small mounded drifts, reflect changing current-flow regimes associated with frontal and water mass evolution, driven by global cooling since the Late Miocene.

Changes in drift texture, mineralogy and provenance

Changes in sediment supply to drift successions include rate changes, compositional changes and textural changes. Steadily increasing the

geographical distance of a site of deposition from a source region will tend to result in a decreasing grain size through time. Changing climate or changing oceanography can result in either grain-size increase or decrease, depending upon the circumstances of a particular case.

The sediment within the Canterbury Drifts changes texture through time (Fig. 12). Between *c*. 21 and 4 Ma, sand content decreased by *c*. 20% at the expense of sortable silt, and cohesive mud increased by *c*. 10%. A further 15% decrease in sand occurred between 4 and 3.1 Ma, after which cohesive mud content increased by up to 33%, again mostly at the expense of sortable silt. Over the same period that these changes occurred, the main sediment mode declined in size from very fine sand in the Early Miocene to coarse silt in the Late Pliocene, and then to abundant very fine silt for the remainder of the succession (Table 1).

The decreasing size of the main sediment mode and increase in cohesive mud that occur through the Canterbury Drifts is consistent with the following known wider changes. First, sediment fining is expected to result from the increasing width of the shelf (transport path) through the Neogene. Second, sediment fining, and enrichment in micas, is expected to have accompanied Neogene uplift along the Alpine Fault plate boundary, which successively exposed higher grade, phyllosilicate-rich metamorphic rocks in the terrestrial source area for the Canterbury Drifts (Carter *et al.* 2004*c*). Third, accelerated uplift during the Early Pliocene, and climatic deterioration from the Late Pliocene on, acted together to encourage the development of montane glaciers in South Island, which greatly increased yields of very fine silt and clay after *c*. 3.1 Ma. This last change is marked also by a rapid rise in chlorite + illite and decrease in smectite within the clay assemblages of nearby DSDP Site 594 (Dersch & Stein 1991) and ODP Site 1123 (Winkler & Dullo 2004).

In summary, the long-term mineralogical and textural trends seen through the Canterbury Drifts were controlled by regional tectonic and climatic events. The trends are consistent with unroofing of basement Rangitata rocks along the South Island mountain spine since the Late Oligocene, which supplied sediment to a continually widening shelf, and with rapid climatic deterioration from the Late Pliocene onwards.

Stratigraphic architecture of the drift body: tectonic implications

The Canterbury Drifts comprise an eastward-thickening, shelf–slope sediment prism *c*. 130 km wide at their widest point in the central basin, *c*. 300 m or less thick at their inner western edge, 2000 m or more thick under the present-day shelf edge in the east and *c*. 400 km long at their seaward edge (Fig. 2a). The volume of this prism is *c*. 60 000 km^3, and since originating in the Late Oligocene (*c*. 24 Ma) it has built seawards at rates between 1 and 5 km Ma^{-1}. Eastward progradation took place into seaward-increasing accommodation (created by the gentle eastward dip of the subjacent Oligocene carbonate platform), and an approximately equal volume of sediment bypassed the inboard prism to be deposited within the Bounty Trough (Carter *et al.* 1994; see Adams 1980, fig. 2).

The Canterbury Drifts are built of sediment fed from mountains along the Alpine Fault plate boundary in western South Island, commencing at *c*. 25 Ma (Carter & Norris 1976). Prior to the Late Miocene, relative motion between the Pacific and Australian plates was dominantly strike-slip, with strong compression and continental collision starting at *c*. 6.4 Ma, since when about 90 km of shortening has occurred in the central Southern Alps (Walcott 1998). None the less, abundant terrigenous sediment was fed eastward from *c*. 24 Ma onwards, indicating that significant transpressive mountains were in existence along the plate boundary throughout the Neogene, despite assertions that development of the Southern Alps as a topographic feature did not occur until the Late Miocene or even Pliocene (Adams & Gabites 1985; Kamp *et al.* 1989; Chamberlain *et al.* 1999). Phases of Southern Alps mountain building can be inferred from peaks in clay mineral trends at 18, 8.5, 6.4, 2.1 and 1.2 Ma (Carter *et al.* 2004*c*, fig. F18).

Adams (1980) has estimated that today about 13×10^9 kg of modern sediment is deposited on the Canterbury shelf and slope each year; that is, *c*. 7.2×10^6 m^3 year^{-1}, assuming an average bulk sediment density of 1.8. Applying such a rate since the onset of plate collision at 6.4 Ma yields a sediment volume of 46 000 km^3, leaving *c*. 12 000 km^3 of the Canterbury Drifts prism to be accounted for by earlier deposition at a rate *c*. 0.68×10^6 m^3 year^{-1}. Outcrop and petroleum well-site information suggest that long-term rates of sediment deposition of 10–15 cm ka^{-1} are characteristic for the drifts that lie beneath the coastal plain and shelf (Carter 1988).

In summary, the Canterbury Drifts are a progradational shelf–slope sediment prism *c*. 400 km long, *c*. 130 km wide and up to 2000 m thick, with an overall volume of *c*. 60 000 km^3. The drifts represent the interaction of an abundant, plate boundary sediment source and major intermediate-depth current flows, and yield a high-resolution record of climatic, oceanographic and tectonic events.

Conclusions

The Canterbury Drifts are of particular interest because of their *c*. 24 Ma longevity, size, deposition at intermediate water depths, and southern mid-latitude location. Regional warping associated with plate boundary tectonics has caused gentle uplift of Late Oligocene–Miocene drifts onland along the western basin margin. Uniquely, therefore, the Canterbury Drifts can be studied in outcrop, in offshore petroleum wells on the shelf, at ODP Site 1119 and DSDP Site 594 on the upper and middle slope, respectively, and in the sea-floor sediments that lie beneath the path of the modern, north-travelling SAMW and AAIW.

Study of the Canterbury Drifts provides insight into the sedimentary characteristics of intermediate-depth drift systems. The drift sediments are dominated by structureless and plane-bedded, polymodal, quartzofeldspathic clayey silts, sandy silts and silty sands, with varying admixtures of benthic and biopelagic carbonate and silica, within which occur intermittent, sharp-based normal-graded and gradational-based double-graded muddy sands, which form up to 10% of the overall drift thickness. The appearance between *c*. 3.2 and 2.0 Ma of a distinctive 9–15 μm grain-size mode is consistent with its origin from glacial grinding processes ('rock-flour'), and the development at that time of uplift and significant montane glaciation on South Island.

The Canterbury Drifts exhibit three seismic signatures. Two display the characteristic mounded shapes and internal sigmoidal bedding that are known from other intermediate- and abyssal-depth sediment drifts (Fig. 3). The two types are differentiated mainly according to their size. A change from larger to smaller drifts at ODP Site 1119 occurred at *c*. 3.1 Ma; that is, at the time that global climate started to deteriorate towards its Pleistocene nadir. Such changes in drift architecture are likely to mark significant changes in oceanographic conditions, and in this case perhaps signal the inception of discrete SAMW flows generated from a newly formed Subantarctic Front located to the south of Site 1119.

Mounded drifts as old as Middle Miocene (*c*. 15 Ma) have been imaged on seismic profiles, and represent climatic deterioration and probably enhanced current flows after that time. The mounded drifts occur enclosed within apparently planar clinoforms of the prograding slope (see Fig. 2). At least some (those along depositional strike from a drift mound) and perhaps all of these clinoforms were deposited under the same northward-moving water masses that built the mounded drifts. Therefore, I infer that a third type of drift signature can be represented by simple clinoform bedding alone. Indeed, Lu *et al.* (2004, fig. 5a) have recently shown that in circumstances where industry-standard seismic profiles resolve only plain clinoform reflectors, higher resolution data yield abundant evidence for a lack of reflector continuity, with minor discordances and lensing consistent with current-influenced deposition. Lu *et al.* concluded (p. 1363) that 'along-strike transport could play a role in forming clinoform morphologies worldwide, even where (seismic) geometries diagnostic of current reworking are lacking'.

Finally, within the Canterbury Drifts the accretion of an individual mounded drift to the upper part of the slope, which occurs by the infilling of its delimiting landward gutter, causes the shelf-edge to 'vault' seawards by several to many kilometres at a time. This episodic type of shelf-edge progradation, together with the possibility that many slope clinoforms may represent contourite drift deposition rather than simple shelf mud-spillover progradation, suggests that a critical appraisal of mechanisms of shelf–slope progradation is overdue.

I thank A. Viana for the invitation to write this paper, and the members of the scientific and technical parties and the crew of R.V. *JOIDES Resolution* for the contributions they made towards the collection, logging and shipboard interpretation of Site 1119 cores on Leg 181. I also thank A. Orpin and C. McKeagney for assistance with grain-size analysis, C. Fulthorpe for providing the seismic lines reproduced in Figures 1 and 3, and J. Howe and J.-C. Faugères for their constructive criticisms of the draft manuscript. This research used samples and data provided by the Ocean Drilling Program (ODP). The ODP is sponsored by the US National Science Foundation (NSF) and participating countries under management of Joint Oceanographic Institutions (JOI), Inc. Financial support was provided by the Australian Research Council (ARC), Grant A-39805139.

Appendix

Grain-size analysis

A total of 220 samples were selected from throughout the Site 1119 succession to characterize the main lithologies and sediment facies present. As a result, sample spacing is at non-systematic intervals. Because of the presence also of core gaps, sample spacing therefore ranges from a few centimetres to 18 m, with an average of 2.33 m.

A total of 108 samples were collected also from the Early Miocene part of the Bluecliffs Formation, the onland representative of the Canterbury Drifts (R. Carter *et al.* 1996). Localities were selected in the south (coast south of Shag River mouth),

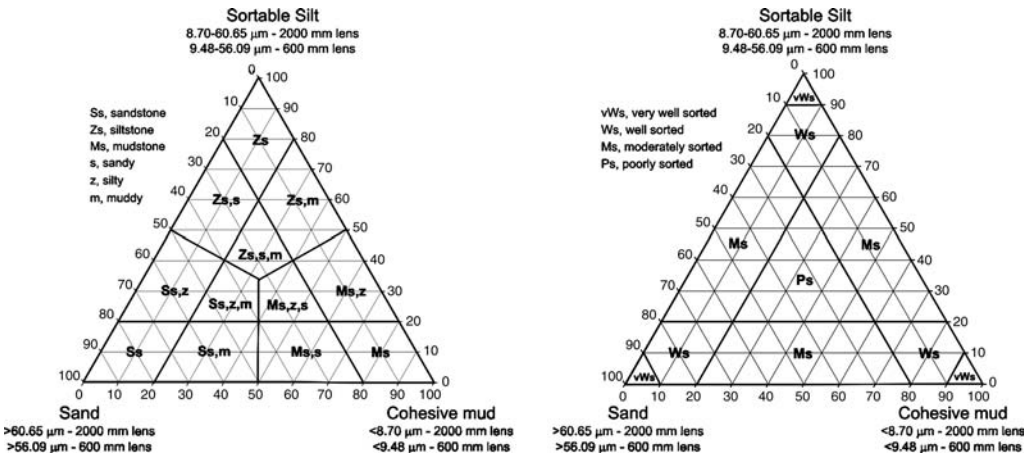

Fig. A1. Sediment type (left) and sorting terminology (right) used in this paper. The cM:sZ:sS compositional space for sediment type is divided into three equal mudstone, siltstone and sandstone fields, with qualifying adjectives delimited by the relevant 20th percentile dividers. Sorting terminology follows similar boundaries.

central (Otaio River; Te Ngawai River) and northern (South Waipara River) parts of the onland Canterbury Basin.

Procedure

Samples were analysed by laser diffraction using a Malvern MasterSizer-X long bed laser particle size analyser. The measurement routine analyses the sample 10 000 times and produces an averaged result processed using a polydisperse algorithm. Depending upon the lens fitted, the particle size distribution is constructed from 32 separate size classes within the range of 1.2–600 μm, or 28 separate size classes within the range of 5–2000 μm. Samples from Site 1119 were analysed using the 600 μm lens; samples from the onshore Bluecliffs Formation, using the 2000 μm lens.

Sediment from each 5 or 10 cm^3 push-core at Site 1119 was gently crumbled into a beaker of tap water, stirred and left to soak for 48 h to ensure complete disaggregation of all sediment particles. To test for complete dispersion of the finer sediment fractions, 15 of the samples between 86 and 115 metres composite depth (mcd), and most of the samples above 86 mcd, were pre-treated with *c*. 10 ml of 30% hydrogen peroxide to remove organic material and allowed to react for at least 36 h. Where appropriate, samples were warmed in a 60 °C water bath to confirm that the reaction had stopped. Samples were then treated again with *c*. 10 ml of 10% glacial acetic acid to remove carbonate material. These samples were left for at least 36 h to react, and, where appropriate, warmed to confirm that all the carbonate had been dissolved.

Samples were dispersed in tap water within a sample bath of *c*. 1 l in volume. When placing the samples into the Malvern sample bath, the entire sample was carefully washed from the beaker. Ultrasonic dispersion was not used. In most cases samples were subjected to vigorous stirring for around 5–10 min, or until the laser obscuration became stable. Laser obscuration was generally maintained in the range 20–50%. Occasional higher obscurations ranged to *c*. 70%, but the results indicate that, provided the samples were well dispersed, accurate and repeatable results are achieved.

A known defect of laser diffraction particle measurement is that erroneous measurement effects occur near the limits of the range of the chosen lens, particularly when a significant amount of the sample is finer-grained than the nominated lens lower limit. In such circumstances, the Malvern controlling software overcompensates by 'squeezing' diffraction data into the finest-grained channels for the lens concerned. This effect produces a spuriously strong sediment mode at around 7 μm for the 2000 mm lens and 2.5 μm for the 600 mm lens. When such spurious peaks are compared with the size distribution of the same sample run using a shorter lens (i.e. more accurate for determining the distribution of very fine silt and clay), the volume per cent of the sample less than 10 μm in diameter (the area beneath the size–frequency plot) is closely similar. Therefore, despite this type of edge effect the Malvern system can be used to make accurate

measurements of the volume per cent of sediment <10 μm, which is why a cutoff as close as possible to that grain diameter was chosen to separate the cohesive mud (cM) and sortable silt (sZ) categories in this study, namely <8.70 or <9.48 μm for the 2000 and 600 mm lens, respectively.

The Bluecliffs Formation samples from onland South Island were subjected to the same laboratory procedure, but analysed using the 2000 μm lens. To allow comparison of grain-size distributions between onland and offshore samples, and because the 2000 μm lens does not give an accurate measurement of clay content, summary statistics for all samples have been calculated using the three categories cohesive mud:'sortable silt':sand (cM:sZ:sS) rather than the conventional clay:silt:sand grain-size classes. The boundary between the cohesive mud (which comprises clay plus very fine silt) and 'sortable silt' categories in nature lies at about 10 μm, corresponding to the grain-size diameter below which fine-grained sediment becomes cohesive and resistant to traction entrainment (McCave 2005). Because the size output classes from the Malvern system do not correspond exactly to traditional geometric grain-size boundaries, and in keeping with the nature of this study, the cohesive mud–sortable silt and sortable silt–sand boundaries were therefore approximated at 8.70 and 60.65 μm (2000 mm lens) and 9.48 and 56.09 μm (600 mm lens), respectively, rather than at the usual clay–silt and silt–sand boundaries of 3.9 and 62.5 μm. Based on these boundary conditions, a pragmatic mud:silt:sand terminology has been used to describe Canterbury Drift sediments (Fig. 12).

A silica 122 μm standard was run for each separate analysis session of around 20 samples to ensure consistent machine performance, and selected samples were reanalysed to ensure that acceptable levels of precision (i.e. closely matching size envelopes) were maintained throughout the periods of analysis.

References

ADAMS, C. J. & GABITES, J. E. 1985. Age of metamorphism and uplift in the Haast Schist Group at Haast Pass, Lake Wanaka and Lake Hawea, South Island, New Zealand. *New Zealand Journal of Geology and Geophysics*, **28**, 85–96.

ADAMS, J. 1980. Contemporary uplift and erosion of the Southern Alps, New Zealand. *Geological Society of America Bulletin*, **91**(1), 1–114.

ANDREWS, P. B. 1963. Stratigraphic nomenclature of the Omihi and Waikari Formations, north Canterbury. *New Zealand Journal of Geology and Geophysics*, **6**, 228–256.

BALLARD, J. A. 1966. Structure of the lower continental rise hills of the western North Atlantic. *Geophysics*, **31**, 506–523.

BISHOP, D. G. & TURNBULL, I. M. (compilers) 1996. Geology of the Dunedin area. *Institute of Geological & Nuclear Sciences (Lower Hutt, New Zealand) 1:250 000 geological map*, **21**.

BUCHANAN, J. 1870. On the Wanganui Beds (upper Tertiary). *Transactions of the New Zealand Institute*, **2**, 163–166.

CARTER, L. & CARTER, R. M. 1988. Late Quaternary development of left-bank-dominant levees in the Bounty Trough, New Zealand. *Marine Geology*, **78**, 185–197.

CARTER, L. & MCCAVE, I. N. 1997. The sedimentary regime beneath the deep western boundary current inflow to the southwest Pacific Ocean. *Journal of Sedimentary Research*, **67**, 1005–1017.

CARTER, L., CARTER, R. M., MCCAVE, I. N. & GAMBLE, J. 1996. Regional sediment recycling in the abyssal Southwest Pacific Ocean. *Geology*, **24**, 735–738.

CARTER, L., CARTER, R. M., NELSON, C. S., FULTHORPE, C. S. & NEIL, H. L. 1990. Evolution of Pliocene to recent abyssal sediment waves on Bounty Channel levees, New Zealand. *Marine Geology*, **95**, 97–109.

CARTER, R. M. 1988. Post-breakup stratigraphy of the Kaikoura Synthem (Cretaceous–Cenozoic), continental margin, southeastern New Zealand. *New Zealand Journal of Geology and Geophysics*, **31**, 405–429.

CARTER, R. M. & GAMMON, P. 2004. New Zealand maritime glaciation: millennial-scale southern climate change since 3.9 Ma. *Science*, **304**, 1659–1662.

CARTER, R. M. & NORRIS, R. J. 1976. Cainozoic history of southern New Zealand: an accord between geological observations and plate-tectonic predictions. *Earth and Planetary Science Letters*, **31**, 85–94.

CARTER, R. M., CARTER, L. & DAVY, B. 1994. Geologic and stratigraphic history of the Bounty Trough, southwestern Pacific Ocean. *Marine and Petroleum Geology*, **11**, 79–93.

CARTER, R. M., CARTER, L. & MCCAVE, I. N. 1996. Current controlled sediment deposition from the shelf to the deep ocean: the Cenozoic evolution of circulation through the SW Pacific gateway. *Geologische Rundschau*, **85**, 438–451.

CARTER, R. M., CARTER, L., WILLIAMS, J. & LANDIS, C. A. 1985. *Modern and relict sedimentation on the Otago continental shelf*. New Zealand Oceanographic Institute, Memoir, **93**.

CARTER, R. M., MCCAVE, I. N., RICHTER, C., *ET AL.* 1999. Southwest Pacific Gateways, Sites 1119–1125. *In*: RICHTER, C., MCCAVE, I. N., CARTER, R. M. & CARTER, L. *ET AL.* (eds) *Proceedings of the Ocean Drilling Program, Initial Reports, 181*, Ocean Drilling Program, (CD-ROM), College Station, TX, 1–80.

CARTER, R. M., FULTHORPE, C. S. & LU, H. 2004*a*. Canterbury Drifts at Ocean Drilling Program Site 1119: climatic modulation of southwest Pacific intermediate water flows since 3.9 Ma. *Geology*, **32**, 1005–1008.

CARTER, R. M., GAMMON, P. R. & MILLWOOD, L. 2004*b*. Glacial–interglacial (MIS 1–10) migrations of the Subtropical Front (STF) across ODP Site 1119, Canterbury Bight, Southwest Pacific Ocean. *Marine Geology*, **205**, 29–58.

CARTER, R. M., MCCAVE, I. N. & CARTER, L. 2004*c*. Fronts, flows, drifts, volcanoes, and the evolution of the southwestern gateway to the Pacific Ocean. *In*: RICHTER, C., MCCAVE, I. N., CARTER, R. M. & CARTER, L. *ET AL.* (eds) *Proceedings of the Ocean Drilling Program, Scientific Results*. Ocean Drilling Program, College Station, TX, 1–110.

CARTER, R. M., NORRIS, R. J. & TURNBULL, I. M. 2005. *The Geology of the Blackmount district, Te Anau–Waiau Basin, western Southland*. Institute of Geological and Nuclear Sciences, Report 2004/123.

CHAMBERLAIN, C. P., POAGE, M. A., CRAW, D. & REYNOLDS, R. C. 1999. Topographic development of the Southern Alps recorded by the isotopic composition of authigenic clay minerals, South Island, New Zealand. *Chemical Geology*, **155**, 279–294.

CHISWELL, S. M. 1996. Variability in the Southland Current, New Zealand. *New Zealand Journal of Marine and Freshwater Research*, **30**, 1–17.

CRAW, D. 1984. Lithologic variations in Otago Schist, Mt Aspiring area, northwest Otago, New Zealand. *New Zealand Journal of Geology and Geophysics*, **27**, 151–166.

DAMUTH, J. E. 1979. Migrating sediment waves created by turbidity currents in the northern South China Basin. *Geology*, **7**, 520–523.

DERSCH, M. & STEIN, R. 1991. Palaoklima und paloozeanische Verhaltnisse im SW-Pazifik wahrend der letzten 6 Millionen Jahre (DSDP—Site 594, Chatham Rucken, ostlich Neuseeland). *Geologische Rundschau*, **80**, 535–556.

DOUGLAS, B. J. 1975. *A paleoenvironmental analysis of a Lower Miocene regressive sequence, upper Tengawai River, South Canterbury, New Zealand*. MSc thesis, University of Otago, Dunedin.

EADE, J. & KENNETT, J. P. 1962. Tertiary sequence at upper Tengawai River, South Canterbury. *New Zealand Journal of Geology and Geophysics*, **5**, 163–174.

EWING, M., EITTREIM, S. A., EWING, J. L. & LE PICHON, S. 1971. Sediment transport and distribution in the Argentine Basin. 3. Nepheloid layer and processes of sedimentation. *Physics and Chemistry of the Earth*, **8**, 49–78.

EXON, N. F., KENNETT, J. P., MALONE, M. J. & Shipboard Scientists 2001. The Tasmanian Gateway: Cenozoic climatic and oceanographic development. *In*: EXON, N. F., KENNETT, J. P. & MALONE, M. J. *ET AL.* (eds) *Proceedings of the Ocean Drilling Program, Initial Reports, 189*. Ocean Drilling Program, College Station, TX, 1–98.

FAUGÈRES, J.-C., GONTHIER, E. & STOW, D. A. V. 1984. Contourite drift molded by deep Mediterranean outflow. *Geology*, **12**, 296–300.

FINLAY, H. J. 1953. Appendix II—Foraminifera. *In*: WELLMAN, H. W. (ed.) *The Geology of the Geraldine Subdivision, S102 Sheet District*, New Zealand Geological Survey, Bulletin, **50**, 47–51.

FLEMING, C. A. 1955. Oceania, Fascicule 4, New Zealand. *Lexique Stratigraphique International*. CNRS, Paris.

FLEMING, C. A. 1962. New Zealand biogeography: a paleontologist's approach. *Tuatara*, **10**(2), 53–108.

FULTHORPE, C. S. & CARTER, R. M. 1991. Continental shelf progradation by sediment drift accretion. *Geological Society of America Bulletin*, **103**, 300–309.

GAGE, M. 1957. *The Geology of the Waitaki Subdivision*. New Zealand Geological Survey, Bulletin, New Series, **55**.

GAIR, H. S. 1959. The Tertiary geology of the Pareora district, south Canterbury. *New Zealand Journal of Geology and Geophysics*, **2**, 265–296.

GARDNER, J. V. & KIDD, R. B. 1987. Sedimentary processes on the northwestern Iberian continental margin viewed by long-range side-scan sonar and seismic data. *Journal of Sedimentary Petrology*, **57**, 397–407.

GULF, 1973. *Basic geophysical data from M.V*. Gulfrex *cruises 94–98, October 1972–January 1973, New Zealand*. New Zealand Geological Survey Open-file Petroleum Report, **614**.

HEATH, R. A. 1972. The Southland Current. *New Zealand Journal of Marine and Freshwater Research*, **6**, 497–533.

HECTOR, J. 1877. *Progress Report*. New Zealand Geological Survey, Reports of Geological Exploration, **1876–77**, iv.

HECTOR, J. 1884. *Progress Report*. New Zealand Geological Survey, Reports of the Geological Explorations **1883–4**, xiii.

HERZER, R. H. 1979. Submarine slides and submarine canyons on the continental slope off Canterbury, New Zealand. *New Zealand Journal of Geology and Geophysics*, **22**, 391–406.

HERZER, R. H. 1981. *Late Quaternary stratigraphy and sedimentation of the Canterbury continental shelf, New Zealand*. New Zealand Oceanographic Institute, Memoirs, **89**.

HERZER, R. H. & LEWIS, D. W. 1979. Growth and burial of a submarine canyon off Motunau, North Canterbury, New Zealand. *Sedimentary Geology*, **24**, 69–83.

HOLLISTER, C. D., FLOOD, R. D., JOHNSON, D. A., LONSDALE, P. & SOUTHARD, J. B. *ET AL.* 1974. Abyssal furrows and hyperbolic echo traces on the Bahama Outer Ridge. *Geology*, **2**, 395–400.

HOWE, J. A., PUDSEY, C. J. & CUNNINGHAM, A. P. 1997. Pliocene–Holocene contourite deposition under the Antarctic Circumpolar Current, Western Falkland Trough, South Atlantic Ocean. *Marine Geology*, **138**, 27–50.

HUTTON, F. W. 1888. On some railway cuttings in the Weka Pass. *Transactions of the New Zealand Institute*, **20**, 262.

JOSEPH, L. H., REA, D. K. & VAN DER PLUIJM, B. A. 2004. Neogene history of the Deep Western Boundary Undercurrent at Rekohu Sediment Drift, Southwest Pacific (ODP Site 1124). *Marine Geology*, **205**, 185–206.

KAMP, P. J. J., GREEN, P. F. & WHITE, S. H. 1989. Fission track analysis reveals character of

collisional tectonics in New Zealand. *Tectonics*, **8**, 169–195.

KIDD, R. B. & HILL, P. R. 1987. Sedimentation on Feni and Gardar sediment drifts. *In*: RUDDIMAN, W. F., KIDD, R. B., THOMAS, E., *ET AL.* (eds) *Initial Reports of the Deep Sea Drilling Project, 94*, US Government Printing Office, Washington, DC, 1217–1244.

KRAUSE, D. C. 1966. *Geology and geomagnetism of the Bounty region, east of South Island, New Zealand*. New Zealand Oceanographic Institute, Memoirs, **30**.

LAUGHTON, A. S., BERGGREN, W. A., *ET AL.* (eds) 1972. *Initial Reports of the Deep Sea Drilling Project, 12*, US Government Printing Office, Washington, DC.

LEMASURIER, W. E. & LANDIS, C. A. 1996. Mantle-plume activity recorded by low-relief erosion surfaces in West Antarctica and New Zealand. *Geological Society of America Bulletin*, **108**, 1450–1466.

LEWIS, D. W., LAIRD, M. G. & POWELL, R. D. 1980. Debris flow deposits of early Miocene age, Deadman Stream, Marlborough, New Zealand. *Sedimentary Geology*, **27**, 83–118.

LONSDALE, P. & HOLLISTER, C. D. 1979. A near-bottom traverse of Rockall Trough: hydrographic and geologic inferences. *Oceanologica Acta*, **2**, 91–106.

LU, H. & FULTHORPE, C. S. 2004. Controls on sequence stratigraphy of a middle Miocene–Holocene, current-swept, passive margin: offshore Canterbury Basin, New Zealand. *Geological Society of America Bulletin*, **116**, 1345–1366.

LU, H., FULTHORPE, C. S. & MANN, P. 2003. Three-dimensional architecture of shelf-building sediment drifts in the offshore Canterbury Basin, New Zealand. *Marine Geology*, **193**, 19–47.

LYNCH-STIEGLITZ, J., FAIRBANKS, R. G. & CHARLES, C. D. 1994. Glacial–interglacial history of Antarctic Intermediate Water: relative strengths of Antarctic versus Indian Ocean sources. *Paleoceanography*, **9**, 7–29.

MASON, B. H. 1941. The geology of Mount Grey District, North Canterbury. *Transactions of the Royal Society of New Zealand*, **71**, 120–122.

MCCAVE, I. N. 2005. Deposition from suspension. *In*: SELLEY, R. C., COCKS, R. & PLIMER, R. (eds) *Encyclopedia of Geology*, **5**. Elsevier, 8–17.

MCCAVE, I. N. & TUCHOLKE, B. E. 1986. Deep current controlled sedimentation in the Western North Atlantic. *In*: VOGT, P. R. & TUCHKOLKE, B. E. (eds) *The Geology of Western North America, V.M., The Western North Atlantic Region*. Geological Society of America, Boulder, CO, 451–468.

MCCAVE, I. N., LONSDALE, P. F., HOLLISTER, C. D. & GARDNER, W. D. 1980. Sediment transport over the Hatton and Gardar contourite drifts. *Journal of Sedimentary Petrology*, **50**, 1049–1062.

MCCAVE, I. N., MANIGHETTI, B. & BEVERIDGE, N. A. S. 1995. Circulation in the glacial North Atlantic inferred from grain-size measurements. *Nature*, **374**, 149–152.

MCCAVE, I. N., MANIGHETTI, B. & ROBINSON, S. G. 1996. Sortable silt and fine sediment size/composition slicing: parameters for palaeocurrent speed and palaeoceanography. *Paleoceanography*, **10**, 593–610.

MILLER, M. C., MCCAVE, I. N. & KOMAR, P. D. 1977. Threshold of sediment motion under unidirectional currents. *Sedimentology*, **24**, 507–528.

MONTADERT, L., ROBERTS, D. G., *ET AL.* (eds) 1979. *Initial Reports of the Deep Sea Drilling Project, 48*. US Government Printing Office, Washington, DC.

MORGANS, H. E. G., EDWARDS, A. R., SCOTT, G. H., *ET AL.* 1999. Integrated biostratigraphy of the Waitakian–Otaian boundary stratotype, Early Miocene, New Zealand. *New Zealand Journal of Geology and Geophysics*, **42**, 581–614.

MORRIS, M., STANTON, B. & NEIL, H. 2001. Sub-antarctic oceanography around New Zealand: preliminary results from an ongoing survey. *New Zealand Journal of Marine and Freshwater Research*, **35**, 499–519.

NELSON, C. H., BARAZA, J. & MALDONADO, A. 1993. Mediterranean undercurrent sandy contourites, Gulf of Cadiz, Spain. *Sedimentary Geology*, **82**, 103–131.

NORMARK, W. R., HESS, G. R., STOW, D. A. V. & BOWEN, A. J. 1980. Sediment waves on the Monterey Fan levee: a preliminary physical interpretation. *Marine Geology*, **37**, 1–18.

REED, J. J. 1957. *Petrology of the Lower Mesozoic rocks of the Wellington district*. New Zealand Geological Survey Bulletin, New Series **57**.

SERANNE, M. & ABEIGNE, C. R. N. 1999. Oligocene to Holocene sediment drifts and bottom currents on the slope of Gabon continental margin (west Africa). Consequences for sedimentation and southeast Atlantic upwelling. *Sedimentary Geology*, **128**, 179–199.

SERVICE, H. 1934. The geology of the Goodwood District, North-east Otago, New Zealand. *New Zealand Journal of Science and Technology*, **15**, 266–274.

STOKER, M. S., AKHURST, M. C., HOWE, J. A. & STOW, D. A. V. 1998. Sediment drifts and contourites on the continental margin off northwest Britain. *Sedimentary Geology*, **115**, 33–51.

STOW, D. A. V. & LOVELL, J. P. B. 1979. Contourites: their recognition in modern and ancient sediments. *Earth-Science Reviews*, **14**, 251–291.

STOW, D. A. V., FAUGÈRES, J.-C. & GONTHIER, E. 1986. Facies distribution and textural variation in Faro Drift contourites: velocity fluctuation and drift growth. *Marine Geology*, **72**, 71–100.

STOW, D. A. V., FAUGÈRES, J.-C., VIANA, A. & GONTHIER, E. 1998. Fossil contourites: a critical review. *Sedimentary Geology*, **115**, 3–31.

SUTTON, P. J. H. 2003. The Southland Current: a sub-antarctic current. *New Zealand Journal of Marine and Freshwater Research*, **37**, 645–652.

VIANA, A. R., FAUGÈRES, J.-C. & STOW, D. A. V. 1998. Bottom-current-controlled sand deposits—a review of modern shallow- to deep-water environments. *Sedimentary Geology*, **115**, 53–80.

WALCOTT, R. I. 1998. Modes of oblique compression: late Cenozoic tectonics of the South Island of New Zealand. *Reviews of Geophysics*, **36**, 1–26.

WARD, D. M. & LEWIS, D. W. 1975. Paleoenvironmental implications of storm-scoured ichnofossiliferous mid-Tertiary limestones, Waihao district, South Canterbury, New Zealand. *New Zealand Journal of Geology and Geophysics*, **18**, 881–908.

WARREN, G. & SPEDEN, I. 1978. *The Piripauan and Haumurian stratotypes (Mata Series, Upper Cretaceous) and correlative sequences in the Haumuri Bluff district, South Marlborough (S56)*. New Zealand Geological Survey Bulletin, **92**.

WESTERN GEOPHYSICAL. 1982. *Final operation report, Canterbury Bight. PPLs 38202 and 38203, BP, Shell, Todd (Canterbury) Services Limited*. New Zealand Geological Survey Open-file Petroleum Report, **898**.

WINKLER, A. & DULLO, W.-C. 2004. Data Report: Miocene to Pleistocene sedimentation pattern on the Chatham Rise, New Zealand. *In*: RICHEER, C., MCCAVE, I. N., CARTER, R. H. & CARTER, L. *ET AL*. (eds) *Proceedings of the Ocean Drilling Program, Scientific Results, 181*. Ocean Drilling Program, College Station, TX (CD-ROM).